receptor/Kirsten rat sarcoma 2 viral oncogene homolog mutation testing to define clonal relationships among multiple lung adenocarcinomas: comparison with clinical guidelines. *Chest* 2010;137:46–52.
337. Nonami Y, Ohtuki Y, Sasaguri S. Study of the diagnostic difference between the clinical diagnostic criteria and results of immunohistochemical staining of multiple primary lung cancers. *J Cardiovasc Surg (Torino)* 2003;44:661–665.
338. Vansteenkiste JF, De Belie B, Deneffe GJ, et al. Practical approach to patients presenting with multiple synchronous suspect lung lesions: a reflection on the current TNM classification based on 54 cases with complete follow-up. *Lung Cancer* 2001;34:169–175.
339. Yoshino I, Nakanishi R, Osaki T, et al. Postoperative prognosis in patients with non-small cell lung cancer with synchronous ipsilateral intrapulmonary metastasis. *Ann Thorac Surg* 1997;64:809–813.
340. Chung JH, Choe G, Jheon S, et al. *Epidermal growth factor receptor* mutation and pathologic-radiologic correlation between multiple lung nodules with ground-glass opacity differentiates multicentric origin from intrapulmonary spread. *J Thorac Oncol* 2009;4:1490–1495.
341. Balak MN, Gong Y, Riely GJ, et al. Novel D761Y and common secondary *T790M* mutations in *epidermal growth factor receptor*-mutant lung adenocarcinomas with acquired resistance to kinase inhibitors. *Clin Cancer Res* 2006;12:6494–6501.
342. Jackman DM, Holmes AJ, Lindeman N, et al. Response and resistance in a non-small-cell lung cancer patient with an epidermal growth factor receptor mutation and leptomeningeal metastases treated with high-dose gefitinib. *J Clin Oncol* 2006;24:4517–4520.
343. Schmid K, Oehl N, Wrba F, et al. *EGFR/KRAS/BRAF* mutations in primary lung adenocarcinomas and corresponding locoregional lymph node metastases. *Clin Cancer Res* 2009;15:4554–4560.
344. Monaco SE, Nikiforova MN, Cieply K, et al. A comparison of *EGFR* and *KRAS* status in primary lung carcinoma and matched metastases. *Hum Pathol* 2010;41:94–102.
345. Meert AP, Martin B, Delmotte P, et al. The role of *EGF-R* expression on patient survival in lung cancer: a systematic review with meta-analysis. *Eur Respir J* 2002;20:975–981.
346. Berghmans T, Paesmans M, Mascaux C, et al. Thyroid transcription factor 1—a new prognostic factor in lung cancer: a meta-analysis. *Ann Oncol* 2006;17:1673–1676.
347. Mascaux C, Iannino N, Martin B, et al. The role of *RAS* oncogene in survival of patients with lung cancer: a systematic review of the literature with meta-analysis. *Br J Cancer* 2005;92:131–139.
348. Nakamura H, Kawasaki N, Taguchi M, et al. Association of HER-2 overexpression with prognosis in nonsmall cell lung carcinoma: a metaanalysis. *Cancer* 2005;103:1865–1873.
349. Mitsudomi T, Hamajima N, Ogawa M, et al. Prognostic significance of p53 alterations in patients with non-small cell lung cancer: a meta-analysis. *Clin Cancer Res* 2000;6:4055–4063.
350. Steels E, Paesmans M, Berghmans T, et al. Role of p53 as a prognostic factor for survival in lung cancer: a systematic review of the literature with a meta-analysis. *Eur Respir J* 2001;18:705–719.
351. Martin B, Paesmans M, Mascaux C, et al. Ki-67 expression and patients survival in lung cancer: systematic review of the literature with meta-analysis. *Br J Cancer* 2004;91:2018–2025.
352. Martin B, Paesmans M, Berghmans T, et al. Role of Bcl-2 as a prognostic factor for survival in lung cancer: a systematic review of the literature with meta-analysis. *Br J Cancer* 2003;89:55–64.
353. Mascaux C, Martin B, Paesmans M, et al. Has Cox-2 a prognostic role in non-small-cell lung cancer? A systematic review of the literature with meta-analysis of the survival results. *Br J Cancer* 2006;95:139–145.
354. Marks JL, Broderick S, Zhou Q, et al. Prognostic and therapeutic implications of *EGFR* and *KRAS* mutations in resected lung adenocarcinoma. *J Thorac Oncol* 2008;3:111–116.
355. Kosaka T, Yatabe Y, Onozato R, et al. Prognostic implication of *EGFR, KRAS,* and *TP53* gene mutations in a large cohort of Japanese patients with surgically treated lung adenocarcinoma. *J Thorac Oncol* 2009;4:22–29.
356. Yanaihara N, Caplen N, Bowman E, et al. Unique microRNA molecular profiles in lung cancer diagnosis and prognosis. *Cancer Cell* 2006;9:189–198.
357. Raponi M, Dossey L, Jatkoe T, et al. MicroRNA classifiers for predicting prognosis of squamous cell lung cancer. *Cancer Res* 2009;69:5776–5783.
358. Hansell DM, Bankier AA, MacMahon H, et al. Fleischner Society: glossary of terms for thoracic imaging. *Radiology* 2008;246:697–722.
359. Godoy MC, Naidich DP. Subsolid pulmonary nodules and the spectrum of peripheral adenocarcinomas of the lung: recommended interim guidelines for assessment and management. *Radiology* 2009;253:606–622.
360. Lee HY, Goo JM, Lee HJ, et al. Usefulness of concurrent reading using thin-section and thick-section CT images in subcentimetre solitary pulmonary nodules. *Clin Radiol* 2009;64:127–132.
361. Takashima S, Sone S, Li F, et al. Small solitary pulmonary nodules (< or =1 cm) detected at population-based CT screening for lung cancer: reliable high-resolution CT features of benign lesions. *AJR Am J Roentgenol* 2003;180:955–964.
362. Ishikawa H, Koizumi N, Morita T, et al. Ultrasmall pulmonary opacities on multidetector-row high-resolution computed tomography: a prospective radiologic-pathologic examination. *J Comput Assist Tomogr* 2005;29:621–625.
363. Kishi K, Homma S, Kurosaki A, et al. Small lung tumors with the size of 1cm or less in diameter: clinical, radiological, and histopathological characteristics. *Lung Cancer* 2004;44:43–51.
364. Kim HY, Shim YM, Lee KS, et al. Persistent pulmonary nodular ground-glass opacity at thin-section CT: histopathologic comparisons. *Radiology* 2007;245:267–275.
365. Kim TJ, Goo JM, Lee KW, et al. Clinical, pathological and thin-section CT features of persistent multiple ground-glass opacity nodules: comparison with solitary ground-glass opacity nodule. *Lung Cancer* 2009;64:171–178.
366. Ikeda K, Awai K, Mori T, et al. Differential diagnosis of ground-glass opacity nodules: CT number analysis by three-dimensional computerized quantification. *Chest* 2007;132:984–990.
367. Choi JA, Kim JH, Hong KT, et al. CT bronchus sign in malignant solitary pulmonary lesions: value in the prediction of cell type. *Eur Radiol* 2000;10:1304–1309.
368. Takashima S, Maruyama Y, Hasegawa M, et al. CT findings and progression of small peripheral lung neoplasms having a replacement growth pattern. *AJR Am J Roentgenol* 2003;180:817–826.
369. Gould MK, Fletcher J, Iannettoni MD, et al. Evaluation of patients with pulmonary nodules: when is it lung cancer?: ACCP evidence-based clinical practice guidelines (2nd edition). *Chest* 2007;132:108S–130S.
370. Nakazono T, Sakao Y, Yamaguchi K, et al. Subtypes of peripheral adenocarcinoma of the lung: differentiation by thin-section CT. *Eur Radiol* 2005;15:1563–1568.
371. Zwirewich CV, Vedal S, Miller RR, et al. Solitary pulmonary nodule: high-resolution CT and radiologic-pathologic correlation. *Radiology* 1991;179:469–476.
372. Yang ZG, Sone S, Takashima S, et al. High-resolution CT analysis of small peripheral lung adenocarcinomas revealed on screening helical CT. *AJR Am J Roentgenol* 2001;176:1399–1407.
373. Tateishi U, Uno H, Yonemori K, et al. Prediction of lung adenocarcinoma without vessel invasion: a CT scan volumetric analysis. *Chest* 2005;128:3276–3283.
374. Kojima Y, Saito H, Sakuma Y, et al. Correlations of thin-section computed tomographic, histopathological, and clinical findings of adenocarcinoma with a bubblelike appearance. *J Comput Assist Tomogr* 2010;34:413–417.
375. Yoshino I, Nakanishi R, Kodate M, et al. Pleural retraction and intra-tumoral air-bronchogram as prognostic factors for stage I pulmonary adenocarcinoma following complete resection. *Int Surg* 2000;85:105–112.
376. Kondo T, Yamada K, Noda K, et al. Radiologic-prognostic correlation in patients with small pulmonary adenocarcinomas. *Lung Cancer* 2002;36:49–57.
377. Sakao Y, Nakazono T, Sakuragi T, et al. Predictive factors for survival in surgically resected clinical IA peripheral adenocarcinoma of the lung. *Ann Thorac Surg* 2004;77:1157–1161.
378. Kuriyama K, Seto M, Kasugai T, et al. Ground-glass opacity on thin-section CT: value in differentiating subtypes of adenocarcinoma of the lung. *AJR Am J Roentgenol* 1999;173:465–469.
379. Castro CY, Coffey DM, Medeiros LJ, et al. Prognostic significance of

percentage of bronchioloalveolar pattern in adenocarcinomas of the lung. *Ann Diagn Pathol* 2001;5:274–284.
380. Hashizume T, Yamada K, Okamoto N, et al. Prognostic significance of thin-section CT scan findings in small-sized lung adenocarcinoma. *Chest* 2008;133:441–447.
381. Dong B, Sato M, Sagawa M, et al. Computed tomographic image comparison between mediastinal and lung windows provides possible prognostic information in patients with small peripheral lung adenocarcinoma. *J Thorac Cardiovasc Surg* 2002;124:1014–1020.
382. Matsuguma H, Yokoi K, Anraku M, et al. Proportion of ground-glass opacity on high-resolution computed tomography in clinical T1 N0 M0 adenocarcinoma of the lung: a predictor of lymph node metastasis. *J Thorac Cardiovasc Surg* 2002;124:278–284.
383. Ohde Y, Nagai K, Yoshida J, et al. The proportion of consolidation to ground-glass opacity on high resolution CT is a good predictor for distinguishing the population of non-invasive peripheral adenocarcinoma. *Lung Cancer* 2003;42:303–310.
384. Okada M, Nishio W, Sakamoto T, et al. Correlation between computed tomographic findings, bronchioloalveolar carcinoma component, and biologic behavior of small-sized lung adenocarcinomas. *J Thorac Cardiovasc Surg* 2004;127:857–861.
385. Sakao Y, Nakazono T, Tomimitsu S, et al. Lung adenocarcinoma can be subtyped according to tumor dimension by computed tomography mediastinal-window setting. Additional size criteria for clinical T1 adenocarcinoma. *Eur J Cardiothorac Surg* 2004;26:1211–1215.
386. Seki N, Sawada S, Nakata M, et al. Lung cancer with localized ground-glass attenuation represents early-stage adenocarcinoma in nonsmokers. *J Thorac Oncol* 2008;3:483–490.
387. Takashima S, Maruyama Y, Hasegawa M, et al. High-resolution CT features: prognostic significance in peripheral lung adenocarcinoma with bronchioloalveolar carcinoma components. *Respiration* 2003;70:36–42.
388. Nishio R, Akata S, Saito K, et al. The ratio of the maximum high attenuation area dimension to the maximum tumor dimension may be an index of the presence of lymph node metastasis in lung adenocarcinomas 3 cm or smaller on high-resolution computed tomography. *J Thorac Oncol* 2007;2:29–33.
389. Shim HS, Park IK, Lee CY, et al. Prognostic significance of visceral pleural invasion in the forthcoming (seventh) edition of TNM classification for lung cancer. *Lung Cancer* 2009;65:161–165.
390. Ikehara M, Saito H, Kondo T, et al. Comparison of thin-section CT and pathological findings in small solid-density type pulmonary adenocarcinoma: prognostic factors from CT findings. *Eur J Radiol*. In press.
391. Gaeta M, Vinci S, Minutoli F, et al. CT and MRI findings of mucin-containing tumors and pseudotumors of the thorax: pictorial review. *Eur Radiol* 2002;12:181–189.
392. Nakata M, Sawada S, Saeki H, et al. Prospective study of thoracoscopic limited resection for ground-glass opacity selected by computed tomography. *Ann Thorac Surg* 2003;75:1601–1605; discussion 5–6.
393. Takashima S, Maruyama Y, Hasegawa M, et al. Prognostic significance of high-resolution CT findings in small peripheral adenocarcinoma of the lung: a retrospective study on 64 patients. *Lung Cancer* 2002;36:289–295.
394. Hiramatsu M, Inagaki T, Matsui Y, et al. Pulmonary ground-glass opacity (GGO) lesions-large size and a history of lung cancer are risk factors for growth. *J Thorac Oncol* 2008;3:1245–1250.
395. Austin JHM, Mujoomdar A, Powell CA, et al. Carcinoma of the lung and metastatic disease of the central nervous system. *Am J Respir Crit Care Med* 2008;178:1090.
396. Mujoomdar A, Austin JHM, Malhotra R, et al. Clinical predictors of metastatic disease to the brain from non-small cell lung carcinoma: primary tumor size, cell type, and lymph node metastases. *Radiology* 2007;242:882–888.
397. MacMahon H, Austin JHM, Gamsu G, et al. Guidelines for management of small pulmonary nodules detected on CT scans: a statement from the Fleischner Society. *Radiology* 2005;237:395–400.
398. Eisenberg RL, Bankier AA, Boiselle PM. Compliance with Fleischner Society guidelines for management of small lung nodules: a survey of 834 radiologists. *Radiology* 2010;255:218–224.
399. MacMahon H. Compliance with Fleischner Society guidelines for management of lung nodules: lessons and opportunities. *Radiology* 2010;255:14–15.
400. Zhao B, James LP, Moskowitz CS, et al. Evaluating variability in tumor measurements from same-day repeat CT scans of patients with non-small cell lung cancer. *Radiology* 2009;252:263–272.
401. Ravenel JG, Leue WM, Nietert PJ, et al. Pulmonary nodule volume: effects of reconstruction parameters on automated measurements—a phantom study. *Radiology* 2008;247:400–408.
402. Jennings SG, Winer-Muram HT, Tarver RD, et al. Lung tumor growth: assessment with CT–comparison of diameter and cross-sectional area with volume measurements. *Radiology* 2004;231:866–871.
403. Winer-Muram HT, Jennings SG, Meyer CA, et al. Effect of varying CT section width on volumetric measurement of lung tumors and application of compensatory equations. *Radiology* 2003;229:184–194.
404. Yankelevitz DF, Reeves AP, Kostis WJ, et al. Small pulmonary nodules: volumetrically determined growth rates based on CT evaluation. *Radiology* 2000;217:251–256.
405. de Hoop B, Gietema H, van de Vorst S, et al. Pulmonary ground-glass nodules: increase in mass as an early indicator of growth. *Radiology* 2010;255:199–206.
406. Nakata M, Sawada S, Yamashita M, et al. Surgical treatments for multiple primary adenocarcinoma of the lung. *Ann Thorac Surg* 2004; 78:1194–1199.
407. Zwirewich CV, Miller RR, Muller NL. Multicentric adenocarcinoma of the lung: CT-pathologic correlation. *Radiology* 1990;176:185–190.
408. Park CM, Goo JM, Kim TJ, et al. Pulmonary nodular ground-glass opacities in patients with extrapulmonary cancers: what is their clinical significance and how can we determine whether they are malignant or benign lesions? *Chest* 2008;133:1402–1409.
409. Okada M, Tauchi S, Iwanaga K, et al. Associations among bronchioloalveolar carcinoma components, positron emission tomographic and computed tomographic findings, and malignant behavior in small lung adenocarcinomas. *J Thorac Cardiovasc Surg* 2007;133:1448–1454.
410. Higashi K, Ueda Y, Seki H, et al. Fluorine-18-FDG PET imaging is negative in bronchioloalveolar lung carcinoma. *J Nucl Med* 1998;39: 1016–1020.
411. Higashi K, Ueda Y, Yagishita M, et al. FDG PET measurement of the proliferative potential of non-small cell lung cancer. *J Nucl Med* 2000;41:85–92.
412. Higashi K, Ueda Y, Ayabe K, et al. FDG PET in the evaluation of the aggressiveness of pulmonary adenocarcinoma: correlation with histopathological features. *Nucl Med Commun* 2000;21:707–714.
413. Ohtsuka T, Nomori H, Watanabe K, et al. Prognostic significance of [(18)F]fluorodeoxyglucose uptake on positron emission tomography in patients with pathologic stage I lung adenocarcinoma. *Cancer* 2006; 107:2468–2473.
414. Raz DJ, Odisho AY, Franc BL, et al. Tumor fluoro-2-deoxy-D-glucose avidity on positron emission tomographic scan predicts mortality in patients with early-stage pure and mixed bronchioloalveolar carcinoma. *J Thorac Cardiovasc Surg* 2006;132:1189–1195.
415. Sagawa M, Higashi K, Sugita M, et al. Fluorodeoxyglucose uptake correlates with the growth pattern of small peripheral pulmonary adenocarcinoma. *Surg Today* 2006;36:230–234.
416. Pastorino U, Landoni C, Marchiano A, et al. Fluorodeoxyglucose uptake measured by positron emission tomography and standardized uptake value predicts long-term survival of CT screening detected lung cancer in heavy smokers. *J Thorac Oncol* 2009;4:1352–1356.
417. Nakayama H, Okumura S, Daisaki H, et al. Value of integrated positron emission tomography revised using a phantom study to evaluate malignancy grade of lung adenocarcinoma: a multicenter study. *Cancer* 2010;116:3170–3177.
418. Um SW, Kim H, Koh WJ, et al. Prognostic value of 18F-FDG uptake on positron emission tomography in patients with pathologic stage I non-small cell lung cancer. *J Thorac Oncol* 2009;4:1331–1336.
419. Berghmans T, Dusart M, Paesmans M, et al. Primary tumor standardized uptake value (SUVmax) measured on fluorodeoxyglucose positron emission tomography (FDG-PET) is of prognostic value for survival in non-small cell lung cancer (NSCLC): a systematic review and meta-analysis (MA) by the European Lung Cancer Working Party for the IASLC Lung Cancer Staging Project. *J Thorac Oncol* 2008;3:6–12.
420. Birchard KR, Hoang JK, Herndon JE Jr, et al. Early changes in tumor size in patients treated for advanced stage nonsmall cell lung cancer do not correlate with survival. *Cancer* 2009;115:581–586.
421. Sohn HJ, Yang YJ, Ryu JS, et al. [18F]Fluorothymidine positron emission tomography before and 7 days after gefitinib treatment pre-

dicts response in patients with advanced adenocarcinoma of the lung. *Clin Cancer Res* 2008;14:7423–7429.
422. Cloran FJ, Banks KP, Song WS, et al. Limitations of dual time point PET in the assessment of lung nodules with low FDG avidity. *Lung Cancer* 2010;68:66–71.
423. Ohno Y, Hatabu H, Takenaka D, et al. Dynamic MR imaging: value of differentiating subtypes of peripheral small adenocarcinoma of the lung. *Eur J Radiol* 2004;52:144–150.
424. van Klaveren RJ, Oudkerk M, Prokop M, et al. Management of lung nodules detected by volume CT scanning. *N Engl J Med* 2009;361: 2221–2229.
425. Oda S, Awai K, Murao K, et al. Computer-aided volumetry of pulmonary nodules exhibiting ground-glass opacity at MDCT. *AJR Am J Roentgenol* 2010;194:398–406.
426. Henschke CI, McCauley DI, Yankelevitz DF, et al. Early Lung Cancer Action Project: overall design and findings from baseline screening. *Lancet* 1999;354:99–105.
427. Henschke CI, Naidich DP, Yankelevitz DF, et al. Early lung cancer action project: initial findings on repeat screenings. *Cancer* 2001;92: 153–159.
428. Lindell RM, Hartman TE, Swensen SJ, et al. Five-year lung cancer screening experience: CT appearance, growth rate, location, and histologic features of 61 lung cancers. *Radiology* 2007;242:555–562.
429. Hasegawa M, Sone S, Takashima S, et al. Growth rate of small lung cancers detected on mass CT screening. *Br J Radiol* 2000;73:1252–1259.
430. Henschke CI, Yankelevitz DF, Libby DM, et al. Survival of patients with stage I lung cancer detected on CT screening. *N Engl J Med* 2006;355:1763–1771.
431. Kakinuma R, Ohmatsu H, Kaneko M, et al. Progression of focal pure ground-glass opacity detected by low-dose helical computed tomography screening for lung cancer. *J Comput Assist Tomogr* 2004;28:17–23.
432. Sone S, Nakayama T, Honda T, et al. Long-term follow-up study of a population-based 1996–1998 mass screening programme for lung cancer using mobile low-dose spiral computed tomography. *Lung Cancer* 2007;58:329–341.
433. Pelosi G, Sonzogni A, Veronesi G, et al. Pathologic and molecular features of screening low-dose computed tomography (LDCT)-detected lung cancer: a baseline and 2-year repeat study. *Lung Cancer* 2008;62:202–214.
434. Wang JC, Sone S, Feng L, et al. Rapidly growing small peripheral lung cancers detected by screening CT: correlation between radiological appearance and pathological features. *Br J Radiol* 2000;73:930–937.
435. Infante M, Cavuto S, Lutman FR, et al. A randomized study of lung cancer screening with spiral computed tomography: three-year results from the DANTE trial. *Am J Respir Crit Care Med* 2009;180:445–453.
436. Bepler G. Are we coming full circle for lung cancer screening a second time? *Am J Respir Crit Care Med* 2009;180:384–385.
437. McMahon PM, Kong CY, Johnson BE, et al. Estimating long-term effectiveness of lung cancer screening in the Mayo CT screening study. *Radiology* 2008;248:278–287.
438. McMahon PM, Kong CY, Weinstein MC, et al. Adopting helical CT screening for lung cancer: potential health consequences during a 15-year period. *Cancer* 2008;113:3440–3449.
439. Gatsonis CA. The National Lung Screening Trial: overview and study design. *Radiology*. 2011;258:243–253.
440. Park EA, Lee HJ, Kim YT, et al. *EGFR* gene copy number in adenocarcinoma of the lung by FISH analysis: investigation of significantly related factors on CT, FDG-PET, and histopathology. *Lung Cancer* 2009;64:179–186.
441. Yano M, Sasaki H, Kobayashi Y, et al. *Epidermal growth factor receptor* gene mutation and computed tomographic findings in peripheral pulmonary adenocarcinoma. *J Thorac Oncol* 2006;1:413–416.
442. Chantranuwat C, Sriuranpong V, Huapai N, et al. Histopathologic characteristics of pulmonary adenocarcinomas with and without *EGFR* mutation. *J Med Assoc Thai* 2005;88(Suppl 4):S322–S329.
443. Huang CT, Yen RF, Cheng MF, et al. Correlation of F-18 fluorodeoxyglucose-positron emission tomography maximal standardized uptake value and *EGFR* mutations in advanced lung adenocarcinoma. *Med Oncol* 2010;27:9–15.
444. Watanabe K, Nomori H, Ohtsuka T, et al. [F-18]Fluorodeoxyglucose positron emission tomography can predict pathological tumor stage and proliferative activity determined by Ki-67 in clinical stage IA lung adenocarcinomas. *Jpn J Clin Oncol* 2006;36:403–409.
445. Vesselle H, Salskov A, Turcotte E, et al. Relationship between non-small cell lung cancer FDG uptake at PET, tumor histology, and Ki-67 proliferation index. *J Thorac Oncol* 2008;3:971–978.
446. Schuchert MJ, Pettiford BL, Keeley S, et al. Anatomic segmentectomy in the treatment of stage I non-small cell lung cancer. *Ann Thorac Surg* 2007;84:926–932.
447. Shapiro M, Weiser TS, Wisnivesky JP, et al. Thoracoscopic segmentectomy compares favorably with thoracoscopic lobectomy for patients with small stage I lung cancer. *J Thorac Cardiovasc Surg* 2009;137: 1388–1393.
448. Yan TD, Black D, Bannon PG, et al. Systematic review and meta-analysis of randomized and nonrandomized trials on safety and efficacy of video-assisted thoracic surgery lobectomy for early-stage non-small-cell lung cancer. *J Clin Oncol* 2009;27:2553–2562.
449. Watanabe T, Okada A, Imakiire T, et al. Intentional limited resection for small peripheral lung cancer based on intraoperative pathologic exploration. *Jpn J Thorac Cardiovasc Surg* 2005;53:29–35.
450. Higashiyama M, Kodama K, Takami K, et al. Intraoperative lavage cytologic analysis of surgical margins in patients undergoing limited surgery for lung cancer. *J Thorac Cardiovasc Surg* 2003;125:101–107.
451. Utsumi T, Sawabata N, Inoue M, et al. Optimal sampling methods for margin cytology examination following lung excision. *Interact Cardiovasc Thorac Surg* 2010;10:434–436.
452. Asamura H, Suzuki K, Watanabe S, et al. A clinicopathological study of resected subcentimeter lung cancers: a favorable prognosis for ground glass opacity lesions. *Ann Thorac Surg* 2003;76:1016–1022.
453. Ginsberg RJ, Rubinstein LV. Randomized trial of lobectomy versus limited resection for T1 N0 non-small cell lung cancer. Lung Cancer Study Group. *Ann Thorac Surg* 1995;60:615–622.
454. Miller DL, Rowland CM, Deschamps C, et al. Surgical treatment of non-small cell lung cancer 1 cm or less in diameter. *Ann Thorac Surg* 2002;73:1545–1550; discussion 50–51.
455. Rami-Porta R, Wittekind C, Goldstraw P. Complete resection in lung cancer surgery: proposed definition. *Lung Cancer* 2005;49:25–33.
456. Ishiguro F, Matsuo K, Fukui T, et al. Effect of selective lymph node dissection based on patterns of lobe-specific lymph node metastases on patient outcome in patients with resectable non-small cell lung cancer: a large-scale retrospective cohort study applying a propensity score. *J Thorac Cardiovasc Surg* 2010;139:1001–1006.
457. Darling GE, Allen MS, Landreneau RJ, et al. Randomized trial of mediastinal lymph node sampling versus complete lymphadenectomy during pulmonary resection in the patient with N0 or N1 (less than hilar) non-small cell carcinoma: results of the ACOSOG Z0030 Trial. *J Thorac Cardiovasc Surg*. In press.
458. Nomori H, Iwatani K, Kobayashi H, et al. Omission of mediastinal lymph node dissection in lung cancer: its techniques and diagnostic procedures. *Ann Thorac Cardiovasc Surg* 2006;12:83–88.
459. Finley DJ, Yoshizawa A, Travis W, et al. Predictors of outcomes after surgical treatment of synchronous primary lung cancers. *J Thorac Oncol* 2010;5:197–205.
460. Hayes DF, Allred C, Anderson BO, et al. Breast. In: SB Edge, DR Byrd, CC Compton, et al. (Eds.). AJCC Cancer Staging Manual, 7th Ed. New York: Springer, 2009. Pp. 347–376.

Lung Cancer xxx (2011) xxx–xxx

Contents lists available at ScienceDirect

Lung Cancer

journal homepage: www.elsevier.com/locate/lungcan

Clinicopathological findings of non-small-cell lung cancer with high serum progastrin-releasing peptide concentrations

Keita Kudo[a], Fumiyoshi Ohyanagi[a], Atushi Horiike[a], Eisaku Miyauchi[a], Noriko Yanagitani[a], Rira Hoshi[c], Yukitoshi Satoh[d], Noriko Motoi[b], Wakako Hamanaka[b], Yuichi Ishikawa[b], Mingyon Mun[a], Yukinori Sakao[a], Sakae Okumura[a], Ken Nakagawa[a], Takeshi Horai[a], Makoto Nishio[a,*]

[a] Thoracic Oncology Center, Cancer Institute Hospital, Japanese Foundation for Cancer Research, 3-8-31 Ariake, Kouto-ku, Tokyo 135-8550, Japan
[b] Department of Pathology, Cancer Institute, Japanese Foundation for Cancer Research, 3-8-31 Ariake, Kouto-ku, Tokyo, Japan
[c] Department of Cytology, Cancer Institute, Japanese Foundation for Cancer Research, 3-8-31 Ariake, Kouto-ku, Tokyo, Japan
[d] Department of Thoracic Surgery, Kitasato University School of Medicine, 1-15-1 Kitasato, Sagamiharashi, Kanagawa, Japan

ARTICLE INFO

Article history:
Received 10 December 2010
Received in revised form 23 March 2011
Accepted 25 March 2011

Keywords:
Non-small-cell lung cancer
Neuroendocrine differentiation
Tumor marker
proGRP
Immunohistochemistry
Chemotherapy

ABSTRACT

Although progastrin-releasing peptide (proGRP) is used as a serum tumor marker for small cell lung cancer (SCLC), high serum pro-GRP concentrations are observed in some non-small-cell lung cancers (NSCLCs). The characteristics of these NSCLCs are not well known. To determine the clinicopathological features of NSCLC in patients with elevated serum proGRP concentrations, serum proGRP values were assessed in 654 advanced lung cancer patients, and positive (>46 pg/mL) NSCLC specimens were subjected to cytological and histopathological reevaluation. Serum proGRP concentrations were positive in 34 of 421 NSCLC patients (8.1%) and 186 of 233 SCLC patients (80%). Histological subtypes of the 34 NSCLC patients at diagnosis were 20 adenocarcinomas, 5 squamous cell carcinomas, 4 large cell carcinomas, and 5 large cell neuroendocrine carcinomas. Six of 27 cytology specimens contained characteristic neuroendocrine morphology. Immunohistochemical analysis showed that 11 of 17 tumors were positive for neuroendocrine markers (64.7%). Twenty of 34 serum proGRP-positive NSCLC patients received platinum-based chemotherapy, and the response rate was 55.0%. These results suggest that serum proGRP-positive NSCLCs may have neuroendocrine differentiation. In addition, serum proGRP-positive NSCLCs may have clinical characteristics that are different from other NSCLCs.

1. Introduction

Lung cancer is the leading cause of cancer death worldwide. In 2005, the number of deaths due to lung cancer in Japan exceeded 60,000 [1]. Conventionally, lung cancer is classified into small cell lung cancer (SCLC) and non-small-cell carcinoma (NSCLC). Because SCLC has neuroendocrine features, it has a poorer prognosis and shows greater sensitivity to chemotherapy than NSCLC. Although NSCLC is subclassified into adenocarcinoma, squamous cell carcinoma, and large cell carcinoma, some NSCLCs have neuroendocrine differentiation. In 1999, the World Health Organization categorized large cell neuroendocrine carcinoma (LCNEC) as a variant of large cell carcinoma [2]. LCNEC has been reported to have a poor prognosis, even for early-stage disease [3,4]. Different types of NSCLCs differ in their clinical behavior according to the presence or absence of neuroendocrine differentiation. Neuroendocrine differentiation in a tumor is generally determined by immunohistochemistry and/or electron microscopy, which reveal the characteristic neuroendocrine morphology [2,5]. However, it is difficult to obtain sufficient tissue by biopsy, and limited tumor tissue sampling may make it difficult to diagnose neuroendocrine differentiation in NSCLC. Therefore, the development of a sensitive serum marker for the detection of neuroendocrine differentiation is greatly desired to facilitate the diagnosis of NSCLCs and neuroendocrine tumors.

Progastrin-releasing peptide (proGRP) is a signal peptide that is produced by small cell lung cancer cells (SCLC). Serum proGRP is considered to be a sensitive tumor marker for SCLC. The sensitivity and specificity of serum proGRP as a tumor marker for SCLC is 60–70% and 96%, respectively [6]. Elevated serum proGRP concentrations have been observed in some NSCLC patients, especially LCNEC patients [6,7], suggesting that serum proGRP is a potentially good marker not only for SCLC but also for NSCLC with neuroendocrine features. However, the clinical and pathological characteristics of NSCLCs with elevated serum proGRP concentrations have not been well studied. In the present study, serum proGRP levels were measured in 654 lung cancer patients and the clinical characteristics of serum proGRP-positive NSCLC patients

* Corresponding author. Tel.: +81 03 3520 0111; fax: +81 03 3570 0343.
E-mail address: mnishio@jfcr.or.jp (M. Nishio).

0169-5002/$ – see front matter © 2011 Elsevier Ireland Ltd. All rights reserved.
doi:10.1016/j.lungcan.2011.03.019

were analyzed; the histopathology of the surgical or biopsy specimens of the positive patients were also evaluated.

2. Patients and methods

Serum proGRP concentrations were measured in 654 patients who were diagnosed with lung cancer by histology or cytology at the Cancer Institute Hospital of the Japanese Foundation for Cancer Research between April 1998 and April 2006.

An enzyme-linked immunosorbent assay (ELISA) kit (serumlabo ProGRP; Fujirebio Diagnostics Inc., Tokyo, Japan) was used to determine serum proGRP concentrations, and samples were considered positive when their values exceeded 46 pg/mL [8].

The clinical characteristics of serum proGRP-positive NSCLC patients were retrospectively analyzed, including age at diagnosis, gender, smoking history, and TNM stage. Response to platinum-based chemotherapy in serum proGRP-positive NSCLC patients was determined according to RECIST criteria (without confirmation).

In addition, the cytological and histological findings of the surgical or biopsy specimens of these patients were reevaluated. Immunohistochemical (IHC) staining was used to evaluate neuroendocrine differentiation in the tumors. Formalin-fixed paraffin-embedded sections were stained for a panel of epithelial markers, including thyroid transcription factor-1 (TTF-1; Dako EnVision+, Saitama, Japan) and carcinoembryonic antigen (CEA; Nichirei, Tokyo, Japan), and neuroendocrine markers, including chromogranin A (CGA) (Dako EnVision+, Saitama, Japan), synaptophysin (Dako EnVision+, Saitama, Japan), CD56 (neural cell adhesion molecule [NCAM]) (Clone 1B6; Novocastra, and proGRP (Advanced Life Science Institute Inc., Saitama, Japan). IHC staining was performed according to standard protocols with EnVision kits (Dako EnVision+, Saitama, Japan). IHC results were grouped into 3 categories – strongly positive, weakly positive, or negative – by well-trained pathologists (WH and NM).

Statistical calculations were performed using StatView version 5.0 for Windows XP (SAS Institute, Cary, NC). Associations between categorical variables and serum proGRP concentrations were evaluated using Student's *t* test. Survival was measured from the start of chemotherapy to the last follow-up evaluation or death, and survival rates were estimated using the Kaplan–Meier method.

3. Results

3.1. Patient characteristics

Of a total of 654 patients, 421 were diagnosed with NSCLC and 233 with SCLC. Serum proGRP samples were positive in 220 of 654 patients, of which 34 (8.1%) had NSCLC and 186 (80%) had SCLC.

The clinical characteristics of serum proGRP-positive and negative NSCLC patients are shown in Table 1. There were no significant differences in the clinical characteristics between the serum proGRP-positive and -negative NSCLC patients.

In serum ProGRP-positive NSCLC patients, the median age of these patients was 67 years (range, 49–77). There were 22 males and 12 females, and 65% of the patients were heavy smokers (smoking index > 400). Most of the patients (94%) had advanced NSCLC. Serum creatinine concentrations were less than 1.6 mg/dL in all 34 serum proGRP-positive NSCLC patients.

The histological subtypes of the 34 serum proGRP-positive NSCLCs at diagnosis were as follows: 20 adenocarcinomas, 5 squamous cell carcinomas, 4 large cell carcinomas, and 5 LCNECs. The rates of positive serum proGRP in each histological subtype were as follows: 7.7% in 260 adenocarcinomas, 5.9% in 85 squamous cell carcinomas, 9.3% in 43 large cell carcinomas, and 44.4% in 11 LCNECs.

Table 1
Clinical characteristics of NSCLC patients.

Characteristics	ProGRP-positive NSCLC patients	ProGRP-negative NSCLC patients
Total no. of patients	34	387
Age, years		
Median (range)	67 (49–77)	62 (29–87)
Sex		
Male/female	22/12	261/126
Smoking index		
Mean (range)	807.5 (0–1400)	661 (0–3000)
Never/≤400/>400	10/2/22	121/29/237
Histological subtype at diagnosis		
Adenocarcinoma	20	240
Squamous cell carcinoma	5	80
Large cell carcinoma	4	48
LCNEC	5	6
Adenosquamous	0	2
Other	0	11
Stage		
I/II	2	56
IIIA	7	63
IIIB	6	106
IV	16	144
Recurrent	3	18

LCNEC: large cell neuroendocrine carcinoma, ProGRP: progastrin-releasing peptide, NSCLC: non-small-cell lung cancer.

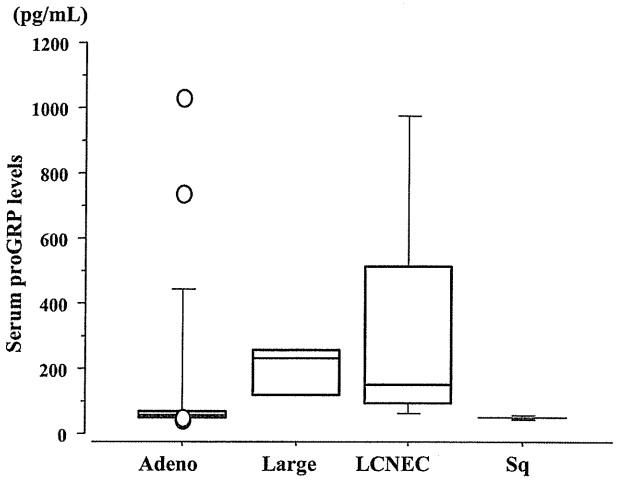

Fig. 1. Serum progastrin-releasing peptide (proGRP) concentrations of 34 non-small-cell lung cancer patients with elevated proGRP. Adeno: adenocarcinoma, Large: large cell carcinoma, LCNEC: large cell neuroendocrine carcinoma, Sq: squamous cell carcinoma.

The median serum proGRP concentration of the 34 NSCLC patients was 60.7 pg/mL and the range was 46.0–973.0 pg/mL. The serum proGRP concentrations in these 34 NSCLC patients were significantly lower than the serum concentrations in proGRP-positive SCLC patients (median, 469 pg/mL; range, 47.1–344,000 pg/mL) ($P < 0.05$).

Fig. 1 shows the serum proGRP concentrations for each histological subtype of serum proGRP-positive NSCLC. The mean serum proGRP concentration in LCNECs was 147 pg/mL and the range was 78.6–973 pg/mL. These concentrations are relatively high compared to other NSCLCs. On the other hand, serum proGRP concentrations were relatively low, even in serum proGRP-positive squamous cell carcinoma patients (median, 47.4 pg/mL; range, 46–56.7 pg/mL).

Table 2
Immunohistochemistry results of non-small-cell lung cancer with elevated serum progastrin-releasing peptide concentrations.

	Serum proGRP (pg/dL)	Histological subtype at diagnosis	Specimen	Stage	IHC					
					TTF-1	CEA	CGA	Synapto-phisin	NCAM	proGRP
1	973	Large	TBLB	IV	–	++	++	++	+	–
2	363	LCNEC	TBLB	IV	++	–	++	++	++	++
3	269	LCNEC	TBLB	IV	++	++	++	++	++	+
4	229	Large	TBLB	IV	–	–	–	–	–	–
5	78.6	Large	TBLB	IV	–	–	–	–	–	–
6	60.3	Adeno	TBLB	IV	++	–	–	–	–	–
7	56.7	Sq	Surgery	Rec	–	+	–	+	++	–
8	56.0	Adeno	Surgery	Rec	++	–	–	+	–	–
9	55.3	Adeno	TBLB	IIIB	++	–	–	+	+	–
10	54.7	Adeno	TBLB	IV	++	–	–	+	–	–
11	53.1	Adeno	Surgery	IB	++	–		+	–	–
12	51.8	Adeno	TBLB	IV	++	+	++	++	++	+
13	51.4	Adeno	Surgery	IB	++	++	++	++	++	++
14	48.3	Sq	TBLB	IB	–	++	–	–	–	–
15	47.4	Sq	Surgery	IIIA	–	++	–	–	–	–
16	47.3	Sq	TBLB	IIIA	–	–	–	+	–	–
17	46	Sq	TBLB	IIIB	–	++	–	–	–	–

IHC: immunohistochemistry, proGRP: progastrin-releasing peptide, TTF-1: thyroid transcription factor 1, CEA: carcinoembryonic antigen, CGA: chromogranin A, NCAM: neural cell adhesion molecule, Adeno: adenocarcinoma, Sq: squamous cell carcinoma, Large: large cell carcinoma, LCNEC: large cell neuroendocrine carcinoma, TBLB: transbronchial lung biopsy, –: negative, +: weakly positive, ++: strongly positive.

3.2. Cytological and histological examination

Cytological specimens corresponding to 27 of the 34 serum proGRP-positive NSCLCs were reevaluated. All 5 cytology specimens diagnosed as LCNEC contained typical neuroendocrine features such as rosette-like and palisading patterns. A rosette-like formation was found in only 1 cytology specimen diagnosed as squamous cell carcinoma, and the other 21 specimens did not contain the typical cytological features of neuroendocrine differentiation.

IHC staining was performed on 17 histological specimens of the 34 serum proGRP-positive NSCLCs (7 adenocarcinomas, 5 squamous cell carcinomas, 3 large cell carcinomas, and 2 LCNECs) to examine neuroendocrine differentiation (Table 2). Four of 17 specimens (24%) showed positive staining (2 weakly and 2 strongly positive) for proGRP, and some neuroendocrine markers were positive in 11 of 17 specimens (64.7%). In particular, 2 of 7 adenocarcinomas, 1 of 3 large cell carcinomas, and 2 of 2 LCNECs showed strongly positive staining for at least 2 out of the 3 neuroendocrine markers CGA, synaptophysin, and NCAM. None of the squamous cell carcinomas showed strongly positive staining for at least 2 out of the 3 neuroendocrine markers CGA, synaptophysin, and NCAM. One of 5 squamous cell carcinomas showed strongly positive staining for NCAM. One of 5 squamous cell carcinomas showed strongly positive staining for NCAM. There was no significant relationship between serum proGRP concentrations and proGRP immunoreactivity.

3.3. Response to chemotherapy

Twenty of 34 serum proGRP-positive NSCLC patients received platinum-based chemotherapy (Table 3). There were 11 partial responses, 4 stable diseases, and no responses observed in the 5 patients. The objective response rate was 55.0%. The median survival of the 20 patients was 11 months, and the 1-year survival rate was 48%.

On the other hand, 232 of 387 serum proGRP-negative NSCLC patients received platinum-based chemotherapy. There were 82 partial responses, 97 stable diseases, and no complete responses observed in the 53 patients. The objective response rate was 35.0%, the median survival was 11.5 months, and the 1-year survival rate was 49.1%.

Table 3
Platinum doublet regimens administered to serum proGRP-positive and -negative patients.

Regimens	ProGRP-positive NSCLC patients ($n=20$)		ProGRP-negative NSCLC patients ($n=232$)	
	n	%	n	%
CBDCA/PTX	9	45	141	60.7
CBDCA/GEM	0	0	16	7
CBDCA/VP16	1	5	5	2
CDDP/DOC	3	15	53	23
CDDP/S-1	2	10	4	1.8
CDDP/VNR	2	10	1	0.5
CDDP/VP16	1	5	0	0
CDDP/CPT11	2	10	2	1
CDDP/GEM	0	0	10	4

CBDCA: carboplatin, CDDP: cisplatin, PTX: paclitaxel, GEM: gemcitabine, VP16: etoposide, DOC: docetaxel, VNR: vinorelbine, CPT11: irinotecan, ProGRP: progastrin-releasing peptide.

4. Discussion

In the present study, the positive rate of serum proGRP concentration in NSCLC patients was 8.1% (34/421), and histological neuroendocrine features were detected in 11 of 17 (64.7%) serum proGRP-positive NSCLC specimens. Several studies have examined serum proGRP concentrations in lung cancer, and all of these studies reported that serum proGRP was a specific tumor marker for SCLC [6,9]. The sensitivity and specificity for SCLCs were around 70% and 99%, respectively, and serum proGRP was superior to NSE [10].

Although increases in serum ProGRP concentration have been observed in some NSCLC patients in previous studies, the reported positive rates of serum proGRP in NSCLCs demonstrated a wide range of variability (3–30%) [6,11]. The 8% positive rate found in the present study was relatively higher than in previous studies, with the exception of 2 reports (the Takada study used a lower cutoff for positive, at 34 pg/mL, and the Molina study included a higher proportion of renal failure patients) [11,12]. Although several studies have reported that serum proGRP values were elevated in NSCLC patients, there have been few studies examining the clinicopathological characteristics of serum proGRP-positive NSCLC patients [13]. Only 1 study examined the clinicopathological

characteristics of 24 NSCLC patients with elevated serum proGRP concentrations. Positive IHC staining for neuroendocrine differentiation was reported in only 4 of 24 serum proGRP-positive NSCLCs, and a small-cell component or neuroendocrine differentiation was detected in all 4 of those patients [13].

In the present study, 27 cytological specimens were reevaluated and IHC staining was performed on 17 histological specimens out of 34 serum proGRP-positive NSCLCs. The cytology results showed the presence of neuroendocrine features such as rosette-like formations in the analysis of 1 squamous cell carcinoma and 5 LCNECs. Histologic examination also identified 2 cases with neuroendocrine morphology (i.e., LCNEC). In addition, weakly or strongly positive staining for some neuroendocrine markers was observed in 12 of 17 histological specimens.

Previous reports have suggested that renal failure can be a source of false-positive proGRP results [11,14], and serum proGRP concentrations were elevated in patients who had serum creatinine levels greater than 1.6 mg/dL [7,13,15]. Therefore, the elevation of serum proGRP detected in present study could be associated with renal dysfunction in the patients analyzed. However, the serum creatinine levels were less than 1.2 mg/dL (median, 0.7 mg/dL) in all 34 serum proGRP-positive NSCLC patients Furthermore, no correlation was observed between serum creatinine and serum proGRP concentrations (data not shown). These results indicate that renal dysfunction could not have accounted for the serum proGRP elevations seen in the present study.

Recently, several reports have suggested that the clinical features of NSCLC with neuroendocrine differentiation, such as LCNEC, may be different from other types of NSCLC [3,16]. The clinical characteristics of serum proGRP-positive NSCLCs were similar to those of SCLCs, as suggested by data showing that the majority of patients were male and heavy smokers. The response rate to platinum-doublet chemotherapy in the present study was 55.0%. This response rate seems higher than the response rates to platinum-doublet chemotherapy reported for nonselected NSCLC [17,18] and serum ProGRP-negative NSCLC in this study, but they were similar to the previously reported response rates to platinum-doublet chemotherapy in LCNEC [16,19]. These results suggest that the sensitivity to chemotherapy in serum proGRP-positive NSCLC may be different than that of other types of NSCLC.

In the present study, IHC staining and a morphologic description were not performed in NSCLC patients with non-elevated proGRP. Therefore, the number of false-negative results and the real performance of the proGRP assay in the detection of neuroendocrine differentiation remain unknown. However, the difficulty in obtaining sufficient tissue by biopsy, and limited tumor tissue sampling make the accurate diagnosis of neuroendocrine differentiation in NSCLC complicated. Sensitive and simple methods for the detection of neuroendocrine differentiation of NSCLC are greatly desired.

In conclusion, serum proGRP-positive NSCLCs may contain manifest neuroendocrine differentiation. In addition, serum proGRP-positive NSCLC patients may have different clinical characteristics compared to other NSCLC patients

Conflict of interest statement

The authors declare no conflicts of interest.

Acknowledgements

The study was conducted by the Cancer Institute Hospital, Japanese Foundation for Cancer Research and Cancer Institute. We thank all investigators in our group.

References

[1] The editorial board of the cancer statistics in Japan. Foundation for Promotion of Cancer Research; October 1, 2007. p. 11–49.
[2] Travis WD, Corrin B, Shimosato Y, Brambilla E.Histological typing of lung and pleural tumors. 3rd ed. Berlin, Heildelberg, Germany: Springer-Verlg; 1999.
[3] Iyoda A, Hiroshima K, Toyozaki T, Haga Y, Fujisawa T, Ohwada H. Clinical characterization of pulmonary large cell neuroendocrine carcinoma and large cell carcinoma with neuroendocrine morphology. Cancer 2001;91: 1992–2000.
[4] Takei H, Asamura H, Maeshima A, Suzuki K, Kondo H, Niki T, et al. Large cell neuroendocrine carcinoma of the lung: a clinicopathologic study of eighty-seven cases. J Thorac Cardiovasc Surg 2002;124:285–92.
[5] Travis WD, Linnoila RI, Tsokos MG, Hitchcock CL, Cutler Jr GB, Nieman L, et al. Neuroendocrine tumors of the lung with proposed criteria for large-cell neuroendocrine carcinoma. An ultrastructural, immunohistochemical, and flow cytometric study of 35 cases. Am J Surg Pathol 1991;15:529–53.
[6] Miyake Y, Kodama T, Yamaguchi K. Pro-gastrin-releasing peptide(31–98) is a specific tumor marker in patients with small cell lung carcinoma. Cancer Res 1994;54:2136–40.
[7] Nakahama H, Tanaka Y, Fujita Y, Fujii M, Sugita M. CYFRA 21-1 and ProGRP, tumor markers of lung cancer, are elevated in chronic renal failure patients. Respirology 1998;3:207–10.
[8] Kodama T, Abe S, Yamaguchi K, Eguchi K, Saigenji K, Kameya T, et al. Clinical significance for diagnosis of serum ProGRP by enzyme-linked immunosorbent assay (ELISA) [in Japanese]. Igaku To Yakugaku 1994;32:87–97.
[9] Holst JJ, Hansen M, Bork E, Schwartz TW. Elevated plasma concentrations of C-flanking gastrin-releasing peptide in small-cell lung cancer. J Clin Oncol 1989;7:1831–8.
[10] Yamaguchi K, Aoyagi K, Urakami K, Fukutani T, Maki N, Yamamoto S, et al. Enzyme-linked immunosorbent assay of pro-gastrin-releasing peptide for small cell lung cancer patients in comparison with neuron-specific enolase measurement. Jpn J Cancer Res 1995;86:698–705.
[11] Molina R, Auge JM, Alicarte J, Filella X, Vinolas N, Ballesta AM. Pro-gastrin-releasing peptide in patients with benign and malignant diseases. Tumour Biol 2004;25:56–61.
[12] Takada M, Kusunoki Y, Masuda N, Matui K, Yana T, Ushijima S, et al. Pro-gastrin-releasing peptide (31–98) as a tumour marker of small-cell lung cancer: comparative evaluation with neuron-specific enolase. Br J Cancer 1996;73:1227–32.
[13] Goto K, Kodama T, Hojo F, Kubota K, Kakinuma R, Matsumoto T, et al. Clinicopathologic characteristics of patients with nonsmall cell lung carcinoma with elevated serum progastrin-releasing peptide levels. Cancer 1998;82: 1056–61.
[14] Casesa A, Filellab X, Molinab R, Ballestab AM, Lopez-Pedreta J, Reverta L. Tumor markers in chronic renal failure and hemodialysis patients. Nephron 1991;57:183–6.
[15] Kamata K, Uchida M, Takeuchi Y, Takahashi E, Sato N, Miyake Y, et al. Increased serum concentrations of pro-gastrin-releasing peptide in patients with renal dysfunction. Nephrol Dial Transplant 1996;11:1267–70.
[16] Fujiwara Y, Sekine I, Tsuta K, Ohe Y, Kunitoh H, Yamamoto N, et al. Effect of platinum combined with irinotecan or paclitaxel against large cell neuroendocrine carcinoma of the lung. Jpn J Clin Oncol 2007;37:482–6.
[17] Ohe Y, Ohashi Y, Kubota K, Tamura T, Nakagawa K, Negoro S, et al. Randomized phase III study of cisplatin plus irinotecan versus carboplatin plus paclitaxel, cisplatin plus gemcitabine, and cisplatin plus vinorelbine for advanced non-small-cell lung cancer: four-arm cooperative study in japan. Ann Oncol 2007;18:317–23.
[18] Schiller JH, Harrington D, Belani CP, Langer C, Sandler A, Krook J, et al. Comparison of four chemotherapy regimens for advanced non–small-cell lung cancer. N Engl J Med 2002;346:92–8.
[19] Yamazaki S, Sekine I, Matsuno Y, Takei H, Yamamoto N, Kunitoh H, et al. Clinical responses of large cell neuroendocrine carcinoma of the lung to cisplatin-based chemotherapy. Lung Cancer 2005;49:217–23.

BJUI BJU INTERNATIONAL

Characteristics and clinical significance of prostate cancers missed by initial transrectal 12-core biopsy

Noboru Numao, Satoru Kawakami, Mizuaki Sakura, Soichiro Yoshida, Fumitaka Koga, Kazutaka Saito, Hitoshi Masuda, Yasuhisa Fujii, Shinya Yamamoto*, Junji Yonese*, Yuichi Ishikawa†, Iwao Fukui* and Kazunori Kihara

*Department of Urology, Graduate School, Tokyo Medical and Dental University, and Departments of *Urology and †Pathology, Cancer Institute Hospital, Japanese Foundation for Cancer Research, Tokyo, Japan*

Accepted for publication 21 April 2011

Study Type – Diagnostic (exploratory cohort)
Level of Evidence 3a

What's known on the subject? and What does the study add?
Initial transrectal 12-core biopsy has a small but definite risk of missing anterior significant prostate cancers irrespective of age, PSA, prostate volume and DRE findings.

Our study yields valuable information for diagnosis and treatment decision of prostate cancer based on transrectal 12-core biopsy.

OBJECTIVE

• To characterize prostate cancers missed by initial transrectal 12-core biopsy.

PATIENTS AND METHODS

• Between 2002 and 2008, 715 men with prostate-specific antigen levels in the range 2.5–20 ng/mL or abnormal digital rectal examination underwent three-dimensional 26-core prostate biopsy (i.e. a combination of transrectal 12-core biopsy and transperineal 14-core biopsy) on initial examination.
• Of the 257 patients diagnosed with cancer, 120 patients subsequently underwent radical prostatectomy.
• Cancers were grouped into TR12-negative cancers (i.e. not detected through transrectal 12-core biopsy but detected through transperineal 14-core biopsy) and TR12-positive (i.e. detected through transrectal 12-core biopsy) cancers.
• Clinicopathological characteristics of the TR12-negative and TR12-positive cancers were evaluated.

RESULTS

• TR12-negative cancers comprised 21% of the three-dimensional 26-core biopsy-detected cancers.
• The frequency of cancers with a biopsy Gleason score ≤6 and that of cancers with a biopsy primary Gleason grade ≤3 was higher in TR12-negative cancers, at 58% and 83%, respectively, than in TR12-positive cancers, at 25% ($P < 0.001$) and 53% ($P < 0.001$), respectively.
• The median number of positive cores in TR12-negative cancers was two out of 26.
• TR12-negative cancers were more frequently located anteriorly than posteriorly.
• The incidence of the TR12-negative cancers was not associated significantly with any clinical variable.

CONCLUSION

• Many of the cancers missed by initial transrectal 12-core biopsy are probably low-grade and low-volume diseases, although initial transrectal 12-core biopsy has a small but definite risk of missing anterior significant cancers.

KEYWORDS

biopsy, prostatectomy, prostatic neoplasm

INTRODUCTION

In a pattern consistent with the worldwide trend toward choosing extended over non-extended prostate biopsy methods, transrectal 12-core prostate biopsy (TR12PBx) is currently one of the most preferred biopsy methods for detecting prostate cancers. A systematic review of prostate biopsy methods noted that TR12PBx strikes a satisfactory balance with sufficiently high rates of cancer detection and sufficiently low rates of biopsy-associated comorbidity, and that taking more than 12 cores adds no significant benefit [1]. TR12PBx also meets the criteria for initial biopsy provided by the representative clinical guidelines [2,3]. Yet several studies have reported that repeat biopsy after negative initial extended transrectal biopsy detects prostate cancer in 17–21% of men [4–6], suggesting that these initial extended transrectal biopsies may miss a substantial number of cancers.

To clarify the incidence and clinical importance of cancers missed by TR12PBx, it is necessary to analyze the results obtained using biopsy protocols that include not only all of the TR12PBx sampling sites, but also

additional sampling sites. To the best of our knowledge, there are currently three biopsy protocols that meet these requirements. The first is three-dimensional 26-core prostate biopsy (3D26PBx), a combination of transperineal 14-core prostate biopsy (TP14PBx) and TR12PBx (Fig. 1), introduced by our group [7–9]. In a previous analysis of 321 men examined through 3D26PBx, we reported that 3D26PBx increased cancer detection by 24% compared to TR12PBx [7]. The second is transrectal 21-core biopsy [10]. The transrectal 21-core biopsy can detect significantly more cancers (increased detection of 9.8%) than the TR12PBx. The third is transrectal 14-core biopsy (TR12PBx plus two extreme anterior apical biopsy sites) [11]. The addition of only two extreme anterior apical sampling sites to TR12PBx increased the cancer detection rate by 7.5%. Although these studies mainly focused on cancer detectability, characteristics of cancers missed by TR12PBx have not been fully assessed to date.

When a patient undergoes an initial TR12PBx and the result is negative for cancer, how much risk does he have for a clinically important cancer that is missed? What are characteristics of the cancers missed by TR12PBx? To address these questions, we evaluated the characteristics of cancers that were detected or missed by TR12PBx in a cohort of 715 men undergoing 3D26PBx.

PATIENTS AND METHODS

PATIENTS

Between June 2002 and June 2008, 757 men prospectively underwent 3D26PBx as an initial biopsy at our institutions because of higher PSA levels >2.5 ng/mL and/or abnormal DRE findings in a clinical setting. Patients were excluded if they had diabetes mellitus or any rectal disease (e.g. uncontrolled hemorrhoids) because of the high risk of infection or rectal bleeding. In principle, those with apparently palpable mass, age ≥75 years, PSA level ≥20 ng/mL or poor state of health were excluded from recommendation for 3D26PBx. Written informed consent was obtained from all patients and 3D26PBx was performed under spinal, general or, recently, local anaesthesia [12], as described previously [7–9]. Of these 757 patients, 42 were excluded from the current study because of palpable stage T3/4 tumours, PSA level ≥20 ng/mL or lack of baseline clinical data. A total of 715 patients were subjected for analyses.

FIG. 1. Transverse, sagittal and coronal projections of three-dimensional 26-core prostate biopsy (3D26PBx), a combination of transperineal 14-core prostate biopsy (TP14PBx) and transrectal 12-core prostate biopsy (TR12PBx). The sampling sites are named: anterior 1 (A1), anterior 2 (A2), posterior 1 (P1), posterior 2 (P2), anterolateral (AL), posterolateral (PL) and transition zone (TZ) in TP14PBx; parasagittal apex (pa), parasagittal midprostate (pm), parasagittal base (pb), lateral apex (la), lateral midprostate (lm) and lateral base (lb) in TR12PBx.

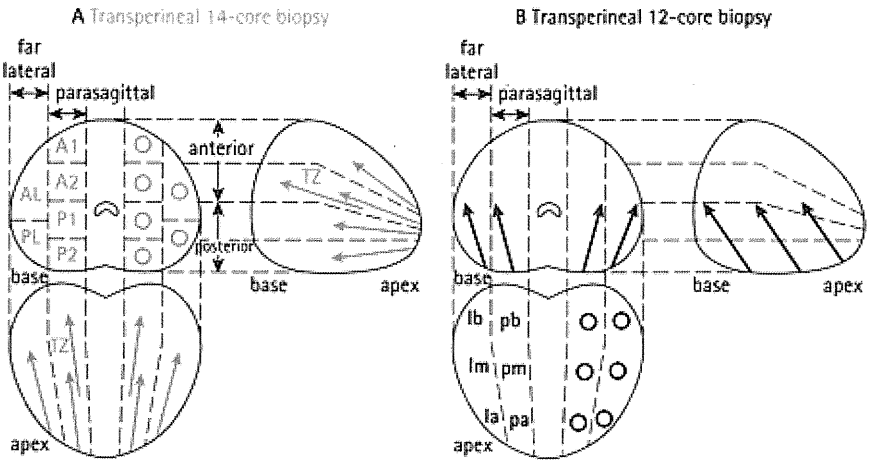

PATHOLOGICAL EVALUATION

All biopsy and radical prostatectomy (RP) specimens were re-evaluated by a single pathologist according to the 2005 International Society of Urologic Pathology Consensus Conference on Gleason Grading [3,13,14]. Each biopsy core was individually labelled so that the location of cancer-positive cores could be analyzed. All RP specimens were processed as described previously [9]. Tumour volume, Gleason score (GS), pathological stage and location of each isolated cancer focus in the RP specimens were recorded. Significant cancer was defined as a tumour volume ≥0.5 mL and/or Gleason pattern 4/5 and/or extraprostatic extension. A significant cancer focus was defined as one fulfilling the above-mentioned criteria for significant cancer, and was extensively evaluated. For analysis of cancer location, the prostate was divided into anterior, posterior and apical regions. The apical region was defined as the most inferior 10 mm of the gland. The remaining part of the gland was divided into anterior and posterior regions at the height of the urethra [15]. When a significant focus lay astride two regions, it was assigned to both regions.

DATA ANALYSIS

All cancers were grouped into two mutually exclusive groups: TR12-negative (i.e. not detected through transrectal 12-core biopsy but detected through transperineal 14-core biopsy) and TR12-positive (i.e. detected through transrectal 12-core biopsy) cancers. The former group did not have cancer-positive cores within the TR12PBx scheme but had cancer-positive cores within the TP14PBx scheme, and the latter had cancer-positive cores within the TR12PBx scheme. These two groups were compared with regard to patient age, PSA level, prostate volume, DRE findings, biopsy GS and the number of positive cores. In patients treated with RP, the two groups were also compared with regard to RP GS, pathological stage, tumour volume, frequency of significant cancer and cancer location. The study cohort was categorized by age, PSA level, prostate volume and DRE findings to identify any patient subgroups in which TR12PBx did not exhibit sufficient cancer detection rates.

STATISTICAL ANALYSIS

All analyses were performed using JMP, version 7 (SAS Institute Inc., Cary, NC, USA). Continuous variables were analyzed using Mann–Whitney's *U*-test. Categorical variables were analyzed using the chi-squared test or Fisher's exact test. The

TABLE 1 Patient and tumour characteristics

Variable	All patients ($n = 715$)	Patients with cancer ($n = 257$)	TR12-positve cancer ($n = 204$)	TR12-negative cancer ($n = 53$)	P
Age (years)	66 (61–71)	66 (63–72)	68 (63–72)	67 (63–73)	0.914
PSA level (ng/mL)	6.1 (4.7–8.5)	7.0 (5.1–9.6)	7.2 (5.1–9.8)	6.8 (5.2–8.7)	0.370
Prostate volume (mL)	35 (27–47)	29 (23–39)	29 (22–37)	32 (27–48)	0.003
% Abnormal DRE	16	25	29	11	0.009
Number of positive cores, *n* (range)	–	5 (2–8)	6 (3–9)	2 (1–2)	<0.001
Biopsy GS, *n* (%)					
5–6	–	83 (32)	52 (25)	31 (58)	<0.001
3 + 4	–	69 (27)	56 (27)	13 (25)	
4 + 3	–	44 (17)	39 (19)	5 (9)	
8 – 10	–	61 (24)	57 (28)	4 (8)	

Continuous variables are expressed as the median (interquartile range). GS, Gleason score; TR12-positive, transrectal 12-core biopsy-positive; TR12-negative, transrectal 12-core biopsy-negative

Transperineal sampling site*	% Cancer detection	P
A1	47	
A2	28	
AL	28	
P1	24	
P2	19	
PL	19	
TZ	19	
A1 + A2	62	0.020†
P1 + P2	40	
A1 + A2 + AL	75	0.009†
P1 + P2 + PL	51	

TABLE 2 TR12-negative cancer ($n = 53$) detection rates in each transperineal sampling site

**See Fig. 1. †According to a chi-squared test (A1 + A2 vs P1 + P2, A1 + A2 + AL vs P1 + P2 + PL). TR12-negative, transrectal 12-core biopsy-negative.*

Cochran–Armitage test was used to test for trends. $P < 0.05$ was considered statistically significant.

RESULTS

CHARACTERISTICS OF TR12-NEGATIVE CANCERS: ANALYSES ON BIOPSY SPECIMENS

Prostate cancers were detected through 3D26PBx in 257 (35.9%) of the 715 men. Of these 257 cancers, 53 (21%) were identified as TR12-negative cancers; in other words, the addition of the TP14PBx sites to the TR12PBx sites improved the cancer detection rate by 26%. Patient and tumour characteristics of TR12-positive and TR12-negative cancers are shown in Table 1. Compared to patients with TR12-positive cancers, patients with TR12-negative cancers had significantly larger prostates and a lower incidence of abnormal DRE. The frequency of cancers with biopsy GS ≤6 and that of cancers with biopsy primary Gleason grade ≤3 were higher in TR12-negative cancers, at 58% and 83%, respectively, than in TR12-positive cancers, at 25% ($P < 0.001$) and 53% ($P < 0.001$), respectively.

In the 53 TR12-negative cancers, cancer-positive rates within the TP14PBx sampling sites are shown in Table 2. The farthest anterior sampling site (A1; Fig. 1) had the highest cancer-positive rate of 47%. There were six cores from the anterior sampling sites (A1, A2 and AL; Fig. 1) that detected significantly ($P = 0.009$) more cancers than six cores from the posterior sites (P1, P2 and PL; Fig. 1), indicating that TR12-negative cancers are located more frequently in the anterior region than in the posterior region.

CHARACTERISTICS OF TR12-NEGATIVE CANCERS: ANALYSES ON RP SPECIMENS

In total, 120 of the 257 (47%) patients underwent RP [16]. Characteristics of TR12-positive and TR12-negative cancers are shown in Table 3. Among the pathological variables analyzed in the RP cohort, the TR12-positive and TR12-negative groups differed with respect to cancer location: specifically, TR12-negative cancers were located less frequently in the posterior region than the TR12-positive cancers.

SUBGROUPS IN WHICH TR12PBX IS INSUFFICIENT FOR CANCER DETECTION

To identify patient subgroups in which TR12PBx would be entirely insufficient for cancer detection and in which more sampling would be needed, we compared the incidence of TR12-negative cancers in subgroups defined by age, PSA level, prostate volume or DRE findings (Fig. 2). Although cancer detection rates of 3D26PBx were significantly higher in patient subgroups with higher age, higher PSA level, smaller prostates or abnormal DRE findings, the incidence of TR12-negative cancers did not differ significantly between any of the subgroups.

COMPARISON OF CANCER CHARACTERISTICS BETWEEN NORMAL AND ABNORMAL DRE GROUPS

PSA screening has significantly increased the proportion of men who undergo prostate biopsy based on PSA findings alone. To evaluate the efficacy of TR12PBx in men with normal DRE in more detail, the cancer characteristics of TR12-negative cancers were analyzed according to DRE findings (Table 4). TR12-positive cancers in the normal DRE group tended to have lower biopsy cancer grade and fewer positive cores compared to those in the abnormal DRE group. By contrast, in TR12-negative cancers, biopsy cancer grade and the number of positive cores did not differ significantly between the groups.

DISCUSSION

In the present study, we evaluated the characteristics of cancers missed by initial TR12PBx, more precisely, cancers missed by TR12PBx in patients who underwent 3D26PBx (TR12-negative cancers), and thus

showed the diagnostic performance of TR12PBx. Initial TR12PBx missed 21% of cancers that were detectable through 3D26PBx; however, it should be noted that more than half of TR12-negative cancers had a biopsy GS ≤6, and most of them had a biopsy primary Gleason grade ≤3. Furthermore, the median number of positive cores in TR12-negative cancers was only two out of 26, suggesting that a substantial number of TR12-negative cancers can be expected to be low-grade and low-volume diseases.

Although our RP cohort is highly selective, most TR12-negative cancers treated with RP were significant cancers. Yet 87% were organ-confined disease and 75% were primary Gleason grade 3 cancers with favourable prognosis. Combined with the biopsy findings, this indicates that TR12-negative cancers have lower malignant potential than TR12-positive cancers, and that most of them can be expected to be organ confined, although a small number of TR12-negative cancers appear to be significant cancers that would exhibit biological aggressiveness.

The characteristics of the location of TR12-negative cancers are clearly shown in the present study. Our analysis of positive transperineal sites in TR12-negative cancers confirmed that TR12-negative cancers were located in the anterior portion of the gland rather than the posterior portion. The cancer location of TR12-negative cancers in RP specimens also supports this notion, suggesting that TR12PBx would be insufficient to detect anterior cancers. The results obtained in the present study are similar to those obtained by Moussa *et al.* [11], who reported that the addition of only two extreme anterior apical cores to TR12PBx transrectal sampling improved cancer detection by 7.5% and that these two cores achieved the highest rate of unique cancer detection. They therefore introduced the 14-core biopsy scheme (TR12PBx biopsy plus two extreme apical cores) as an initial biopsy to detect more anterior apical cancers.

On the basis of these findings, simply adding more transrectal sampling sites from the bottom of the prostate gland to TR12PBx would not increase its cancer detection rate efficiently. Indeed, several studies have tested transrectal extended biopsy methods using more than 12 cores; however, most of these so-called 'saturation' transrectal biopsy protocols did not outperform TR12PBx [17–19]. The transrectal 21-core biopsy [10] can identify more cancers than TR12PBx can, although the 9.8% increase in cancer detection that results from the nine additional samplings appears to be inefficient. In the present study, the addition of two far-anterior transperineal sampling to the TR12PBx improved its cancer detection rate by 11%. From these results, we consider that a few additional samplings in the anterior apical portion are effective for detecting cancers missed by TR12PBx.

In recent analyses on men with a PSA level <20 ng/mL without locally advanced tumours on DRE findings, there were no significant differences among subgroups defined by age, PSA level, prostate volume or DRE in the incidence of TR12-negative cancers. Therefore, we could not identify any subgroup in which TR12PBx would be entirely insufficient for cancer detection and in which more sampling would therefore be needed. There is the potential concern that TR12PBx may probably miss anterior aggressive cancers in men with normal DRE, although our analysis of cancer characteristics according to DRE findings shows that a large proportion of TR12-negative cancers probably consist of low-grade and low-volume disease, regardless of DRE findings. We consider that these results are sufficient grounds to eliminate such concerns.

Recently, the value of MRI for detecting prostate cancers and determining their location has been extensively studied [20]. Lawrentschuk *et al.* [21] retrospectively analyzed patients with anteriorly predominant tumours on MRI who had undergone prostate biopsy and reported that MRI would be useful in the detection of

TABLE 3 Patient and tumour characteristics of 120 men undergoing radical prostatectomy

Variable	TR12-positive cancer (n = 104/204)	TR12-negative cancer (n = 16/53)	P
Clinical			
Age (years)	67 (62–71)	64 (60–70)	0.245
PSA level (ng/mL)	6.7 (5.2–9.3)	6.4 (4.7–8.4)	0.362
Prostate volume (mL)	28 (22–34)	29 (20–38)	0.817
% Abnormal DRE	24	25	0.666
Biopsy			
Number of positive cores, n (range)	5 (3–9)	2 (1–3)	<0.001
GS, n (%)			
5–6	17 (16)	8 (50)	<0.001
3 + 4	32 (31)	5 (31)	
4 + 3	27 (26)	1 (6)	
8–10	28 (27)	2 (13)	
Radical prostatectomy			
GS, n (%)			
5–6	26 (25)	3 (19)	<0.001
3 + 4	49 (47)	9 (56)	
4 + 3	16 (15)	3 (19)	
8–10	13 (13)	1 (6)	
% Organ-confined disease	73	87	0.178
% Tumour volume ≥0.5 mL	80	75	0.437
% Significant cancer	92	87	0.396
Significant cancer			
% Located posteriorly	83	50	<0.001
% Located anteriorly	75	71	0.500
% Located apically	86	79	0.331

Continuous variables are expressed as the median (interquartile range). GS, Gleason score; TR12-positive, transrectal 12-core biopsy-positive; TR12-negative, transrectal 12-core biopsy-negative.

anterior tumours that are difficult to detect using transrectal biopsy. It appears that MRI is a promising tool for detecting anterior cancers, although its cost is high.

Pathological evaluation in the present study is based on the 2005 International Society of Urologic Pathology Consensus [13,14]. Fused glands, ill-defined glands with poorly formed glandular lumina and most of the cribriforms are previously categorized into Gleason pattern 3 but, in the 2005 consensus, are categorized into Gleason pattern 4. Furthermore, two new modifications to the Gleason scoring system are recommended in the evaluation of biopsy specimens. One is that any high-grade pattern, no matter how small quantitatively, should be incorporated into the GS, although any secondary grade that occupies <5% of the specimen would not have been reported under the previous system. The other modification is that all higher tertiary grade components of the tumour, which were previously ignored, should be incorporated into the GS. Accordingly, the rates of high-grade patterns scored according to the 2005 consensus are higher than those scored under the previous system. This phenomenon has been confirmed in a study by Billis *et al.* [22] showing that GS that had been scored under the previous system were upgraded by re-evaluation under the 2005 consensus in 26.7% of the biopsy specimens. Similarly, the GS of some of the patients in the present study would have been lower if they had been evaluated under the previous system. We consider that these findings strengthen our view that many TR12-negative cancers can be expected to be low-grade diseases.

FIG. 2. Bar graphs show detection rates of cancers of all types through 3D26PBx. The overlying line plots show detection rates of TR12-negative cancers (i.e. not detected through transrectal 12-core biopsy but detected through transperineal 14-core biopsy). Statistical analyses were performed using the Cochran–Armitage trend test.

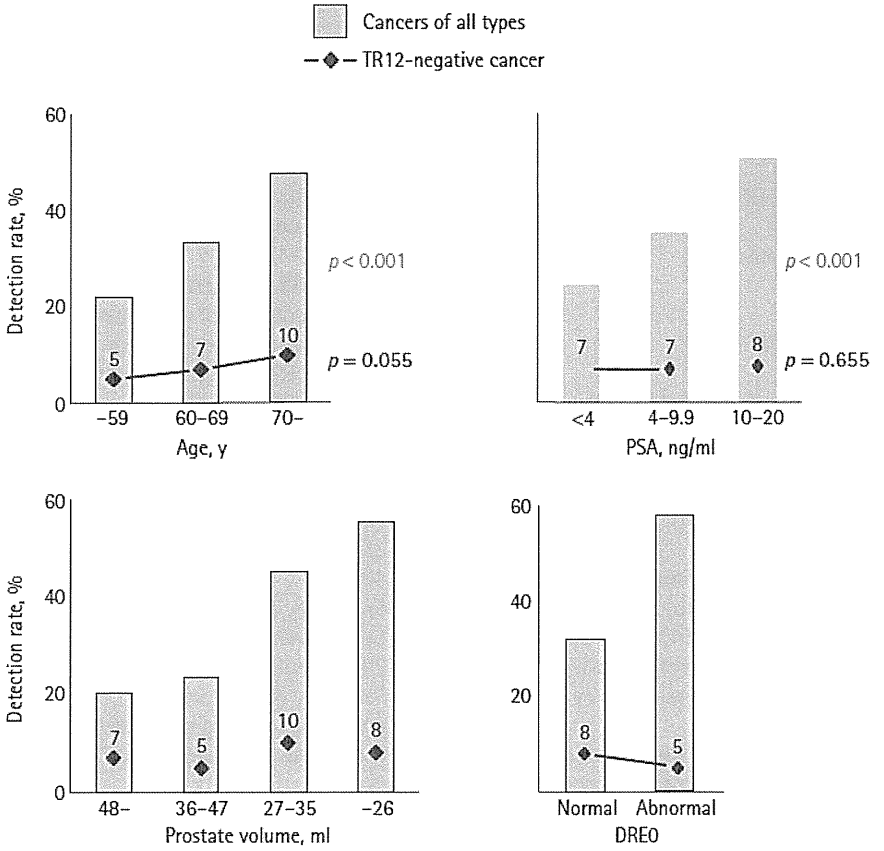

The present study does not indicate that we should aim to actively detect TR12-negative cancers in all candidates for initial prostate biopsy because a substantial number of TR12-negative cancers are low-grade and low-volume diseases. Overdiagnosis and

overtreatment are now issues of major concern in the management of prostate cancer. Draisma *et al.* [23] have reported that the rate of overdiagnosis of prostate cancer has been estimated at 23–66% of screening-detected cancers. The main purpose of prostate biopsy is not only to detect more prostate cancers, but also to detect more life-threatening cancers. Even if we missed a case of prostate cancer at an initial biopsy, we would be able to determine the need for a repeat biopsy through the PSA test in most cases, and most cancers detected by repeat biopsy are manageable and not life-threatening [24]. If the goal of screening were simply to detect life-threatening cancers, the addition of sampling sites to the TR12PBx protocol would not be essential in all candidates for initial biopsy.

Another important purpose of biopsy, however, is to accurately characterize any tumours to allow for a more informed treatment decision-making process. If a custom treatment is to be devised for each individual patient, more sampling is required to generate more information, although more sampling leads to a greater detection of indolent cancers. This clinical dilemma makes it difficult to determine the optimal biopsy scheme. We now consider that the addition of anterior sampling sites to the initial TR12PBx would be a reasonable option for younger men with a long life expectancy or for men with suspected anterior cancer as assessed by MRI. On the basis of the analysis in subgroups divided by DRE findings, the finding that a DRE was normal does not mean that additional sampling of the anterior prostate should be performed. At repeat biopsy after negative TR12PBx, however, anterior samplings are highly recommended.

The present study has several limitations that should be considered. Given that 3D26PBx does not identify all cancers, it is possible that TP12PBx may fail to detect an even greater percentage of cancers than reported in the present study. We recommend transperineal sampling for the detection of TR12-negative cancers, although we realize that the transperineal approach may be unfamiliar to many urologists. A recently reported technique for simple and effective local anaesthesia would render transperineal extended biopsy more feasible [12]. Furthermore, because of the limited duration of the follow-up in the present study, we could not report the oncological outcome of TR12-negative cancers. Long-term observation will be required to acquire a better understanding of the diagnostic performance of TR12PBx.

In conclusion, TR12PBx missed 21% of cancers that were detected by 3D26PBx on initial biopsy. Although many of the undetected cancers were expected to be low-grade and low-volume diseases, it should be noted that the initial TR12PBx has a small but definite risk of missing anterior significant cancers.

CONFLICT OF INTEREST

None declared.

REFERENCES

1 **Eichler K, Hempel S, Wilby J, Myers L, Bachmann LM, Kleijnen J.** Diagnostic value of systematic biopsy methods in the investigation of prostate cancer: a systematic review. *J Urol* 2006; **175**: 1605–12

2 **NCCN Clinical Practice Guideline in Oncology.** Prostate Cancer Early Detection. V.2.2010. Available at: http://www.nccn.org/professionals/physician_gls/f_guidelines.asp. Accessed October 2010

3 **Heidenreich A, Bolla M, Joniau S *et al.*** Guidelines on Prostate Cancer 2010. Available at: http://www.uroweb.org/gls/pdf/08_Prostate_Cancer.pdf. Accessed October 2010

4 **Campos-Fernandes JL, Bastien L, Nicolaiew N *et al.*** Prostate cancer detection rate in patients with repeated extended 21-sample needle biopsy. *Eur Urol* 2009; **55**: 600–6

5 **Philip J, Hanchanale V, Foster CS, Javlé P.** Importance of peripheral biopsies in maximising the detection of early prostate cancer in repeat 12-core biopsy protocols. *BJU Int* 2006; **98**: 559–62

6 **Singh H, Canto EI, Shariat SF *et al.*** Predictors of prostate cancer after initial negative systematic 12 core biopsy. *J Urol* 2004; **171**: 1850–4

7 **Kawakami S, Hyochi N, Yonese J *et al.*** Three-dimensional combination of transrectal and transperineal biopsies for efficient detection of stage T1c prostate cancer. *Int J Clin Oncol* 2006; **11**: 127–32

8 **Kawakami S, Okuno T, Yonese J *et al.*** Optimal sampling sites for repeat prostate biopsy: a recursive partitioning analysis of three-dimensional 26-core systematic biopsy. *Eur Urol* 2007; **51**: 675–82

9 **Numao N, Kawakami S, Yokoyama M *et al.*** Improved accuracy in predicting the presence of Gleason pattern 4/5 prostate cancer by three-dimensional 26-core systematic biopsy. *Eur Urol* 2007; **52**: 1663–8

10 **Guichard G, Larré S, Gallina A *et al.*** Extended 21-sample needle biopsy protocol for diagnosis of prostate cancer in 1000 consecutive patients. *Eur Urol* 2007; **52**: 430–5

11 **Moussa AS, Meshref A, Schoenfield L *et al.*** Importance of additional 'extreme' anterior apical needle biopsies in the initial detection of prostate cancer. *Urology* 2010; **75**: 1034–9

12 **Kubo Y, Kawakami S, Numao N *et al.*** Simple and effective local anesthesia for transperineal extended prostate biopsy: application to three-dimensional 26-core biopsy. *Int J Urol* 2009; **16**: 420–3

13 **Epstein JI, Allsbrook WC Jr, Amin MB, LL E, Grading ISUP.** Committee. The 2005 International Society of Urological Pathology (ISUP) Consensus Conference on Gleason Grading of Prostatic Carcinoma. *Am J Surg Pathol* 2005; **29**: 1228–42

14 **Srigley JR, Amin MB, Epstein JI *et al.*** Updated protocol for the examination of specimens from patients with carcinomas of the prostate gland. *Arch Pathol Lab Med* 2006; **130**: 936–46

15 **Koppie TM, Bianco FJ Jr, Kuroiwa K *et al.*** The clinical features of anterior prostate cancers. *BJU Int* 2006; **98**: 1167–71

16 **Kawakami S, Fukui I, Yonese J *et al.*** Antegrade radical retropubic prostatectomy with preliminary ligation of vascular pedicles in 614 consecutive patients. *Jpn J Clin Oncol* 2007; **37**: 528–33

17 **Jones JS, Patel A, Schoenfield L, Rabets JC, Zippe CD, Magi-Galluzzi C.** Saturation technique does not improve cancer detection as an initial prostate biopsy strategy. *J Urol* 2006; **175**: 485–8

18 **Pepe P, Aragona F.** Saturation prostate needle biopsy and prostate cancer detection at initial and repeat evaluation. *Urology* 2007; **70**: 1131–5
19 **Scattoni V, Roscigno M, Raber M *et al.*** Initial extended transrectal prostate biopsy – are more prostate cancers detected with 18 cores than with 12 cores? *J Urol* 2008; **179**: 1327–31
20 **Villers A, Puech P, Mouton D, Leroy X, Ballereau C, Lemaitre L.** Dynamic contrast enhanced, pelvic phased array magnetic resonance imaging of localized prostate cancer for predicting tumor volume: correlation with radical prostatectomy findings. *J Urol* 2006; **176**: 2432–7
21 **Lawrentschuk N, Haider MA, Daljeet N *et al.*** 'Prostatic evasive anterior tumours': the role of magnetic resonance imaging. *BJU Int* 2010; **105**: 1231–6
22 **Billis A, Guimaraes MS, Freitas LL, Meirelles L, Magna LA, Ferreira U.** The impact of the 2005 international society of urological pathology consensus conference on standard Gleason grading of prostatic carcinoma in needle biopsies. *J Urol* 2008; **180**: 548–52
23 **Draisma G, Etzioni R, Tsodikov A *et al.*** Lead time and overdiagnosis in prostate-specific antigen screening: importance of methods and context. *J Natl Cancer Inst* 2009; **101**: 374–83
24 **Schröder FH, van den Bergh RC, Wolters T *et al.*** Eleven-year outcome of patients with prostate cancers diagnosed during screening after initial negative sextant biopsies. *Eur Urol* 2010; **57**: 256–66

Correspondence: Noboru Numao, Department of Urology, Tokyo Medical and Dental University Graduate School, 1-5-45 Yushima, Bunkyo-ku, Tokyo 113-8519, Japan.
e-mail: noboru.uro@tmd.ac.jp

Abbreviations: **3D26PBx**, three-dimensional 26-core prostate biopsy; **GS**, Gleason score; **RP**, radical prostatectomy; **TR12PBx**, transrectal 12-core prostate biopsy; **TP14PBx**, transperineal 14-core prostate biopsy.

nature medicine

RET, ROS1 and ALK fusions in lung cancer

Kengo Takeuchi[1,2], Manabu Soda[3], Yuki Togashi[1,2], Ritsuro Suzuki[4], Seiji Sakata[1], Satoko Hatano[1], Reimi Asaka[1,2], Wakako Hamanaka[2], Hironori Ninomiya[2], Hirofumi Uehara[5], Young Lim Choi[6], Yukitoshi Satoh[5,7], Sakae Okumura[5], Ken Nakagawa[5], Hiroyuki Mano[3,6] & Yuichi Ishikawa[2]

Through an integrated molecular- and histopathology-based screening system, we performed a screening for fusions of anaplastic lymphoma kinase (ALK) and c-ros oncogene 1, receptor tyrosine kinase (ROS1) in 1,529 lung cancers and identified 44 ALK-fusion–positive and 13 ROS1-fusion–positive adenocarcinomas, including for unidentified fusion partners for ROS1. In addition, we discovered previously unidentified kinase fusions that may be promising for molecular-targeted therapy, kinesin family member 5B (KIF5B)-ret proto-oncogene (RET) and coiled-coil domain containing 6 (CCDC6)-RET, in 14 adenocarcinomas. A multivariate analysis of 1,116 adenocarcinomas containing these 71 kinase-fusion–positive adenocarcinomas identified four independent factors that are indicators of poor prognosis: age ≥50 years, male sex, high pathological stage and negative kinase-fusion status.

Echinoderm microtubule associated protein like 4 (EML4)-ALK was the first targetable fusion oncokinase to be identified in non–small cell lung cancer (NSCLC)[1]. This fusion is found in approximately 4–6% of lung adenocarcinomas[2,3]. ROS1 is another receptor tyrosine kinase that forms fusions in NSCLC[4]. Solute carrier family 34 (sodium phosphate), member 2 (SLC34A2)-ROS1 and CD74 molecule, major histocompatibility complex, class II invariant chain (CD74)-ROS1 were identified in 1 out of 41 NSCLC cell lines and 1 out of 150 lung cancer samples, respectively[4]. However, the oncogenic ability of these ROS1 fusion proteins and the incidence of ROS1 fusions in lung cancers are still unclear.

We screened for known and unknown kinase fusions in lung cancers using a histopathology-based system with tissue microarrays of 1,528 surgically removed tissues (**Supplementary Methods** and **Supplementary Appendix**). Immunohistochemistry of antibodies to ALK using the intercalated antibody-enhanced polymer method[2,3,5–7] detected 45 tumors with ALK kinase domain expression (**Supplementary Fig. 1**). In 44 adenocarcinomas, multiplex RT-PCR[2,3] identified 41 *EML4-ALK*–positive and 3 *KIF5B-ALK*–positive adenocarcinomas, including a previously unidentified KIF5B-ALK fusion variant, K17;A20 (**Supplementary Table 1**). Further, we used fluorescence *in situ* hybridization (FISH) for split and fusion assays to confirm the presence of ALK fusions[2,3,8]. The FISH results for the *ALK* split assay, the *EML4-ALK* fusion assay and the *KIF5B-ALK* fusion assay in the 44 adenocarcinomas were all consistent with the presence of the corresponding fusion gene (**Supplementary Figs. 2** and **3**). The remaining tumor that was positive for antibodies to ALK as determined by immunohistochemistry (a large-cell neuroendocrine carcinoma) was negative in the FISH assays and expressed wild-type ALK. ALK fusions existed in 3.0% (44 out of 1,485) of the NSCLCs and 3.9% (44 out of 1,121) of the adenocarcinomas. We included 20 previously reported ALK-fusion–positive and 304 ALK-fusion–negative tumors, all of which were screened with multiplex RT-PCR. Because specimens of these 324 patients were collected consecutively during the period of tissue collection, they served as positive and negative controls, respectively[1–3,8,9]. The immunohistochemistry results using the intercalated antibody-enhanced polymer method were complete matches in the 20 fusion-positive and the 304 fusion-negative tumors.

We used split FISH assays for the screening for *ROS1* gene rearrangement (**Fig. 1**). In 11 of the 13 *ROS1* split FISH-positive tumors (**Fig. 1a**), 5′ rapid amplification of complementary DNA ends (5′ RACE) identified two known and three unknown fusion partners for *ROS1*: *TPM3*, *SDC4*, *SLC34A2*, *CD74* and *EZR* (**Fig. 1b** and **Supplementary Table 1**); RT-PCR confirmed this finding (**Fig. 1c**). In a 5′-RACE–negative tumor (ROS#12) (again, where split FISH is used to detect candidate fusion genes of interest by the presence of rearrangements and RACE is used for the identification of fusion partners), each fusion-specific RT-PCR (using a common reverse primer) amplified the same band, which contained an *LRIG3* sequence. This tumor was proven fusion-positive in RT-PCR specific to *LRIG3-ROS1*, an unidentified fusion. Fusion FISH results confirmed that all 12 cases harbored the corresponding fusion (**Fig. 1a**). All fusion FISH assays for these six ROS1 fusions were negative for the tumor ROS#13 (the frozen material had been consumed), indicating an unknown fusion partner for *ROS1*. *ROS1* split FISH screening failed for nine NSCLCs, including five adenocarcinomas. We identified ROS1 fusions in 0.9% (13 out of 1,476) of the NSCLCs and 1.2% (13 out of 1,116) of the adenocarcinomas.

We performed *KIF5B* split FISH to discover new fusion kinases, as we previously identified KIF5B-ALK fusions in lung cancer[3]. As such, we hypothesized that KIF5B might be rearranged in lung cancer. In 24 *KIF5B* split FISH-positive tumors, 3′ RACE identified an in-frame fusion between *KIF5B* exon 23 and *RET* exon 12

[1]Pathology Project for Molecular Targets, the Cancer Institute, Japanese Foundation for Cancer Research, Tokyo, Japan. [2]Division of Pathology, the Cancer Institute, Japanese Foundation for Cancer Research, Tokyo, Japan. [3]Division of Functional Genomics, Jichi Medical University, Tochigi, Japan. [4]Department of Hematopoietic Stem Cell Transplantation Data Management and Biostatistics, Nagoya University Graduate School of Medicine, Nagoya, Japan. [5]Department of Thoracic Surgical Oncology, Thoracic Center, the Cancer Institute Hospital, Japanese Foundation for Cancer Research, Tokyo, Japan. [6]Department of Medical Genomics, Graduate School of Medicine, University of Tokyo, Tokyo, Japan. [7]Present address: Department of Thoracic Surgery, Kitasato University School of Medicine, Kanagawa, Japan. Correspondence should be addressed to K.T. (kentakeuchi-tky@umin.net).

Received 28 September 2011; accepted 3 January 2012; published online 12 February 2012; doi:10.1038/nm.2658

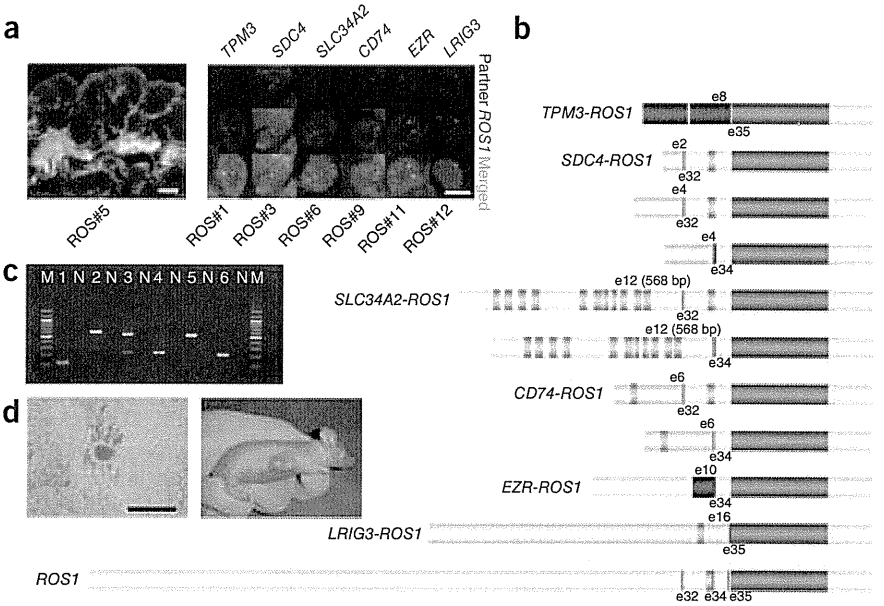

Figure 1 Identification of ROS1 fusions. (**a**) *ROS1* split (left) and fusion (right) FISH assay data (scale bars, 20 μm). In the split assay, multiple tumor cells harbored individual 3′ side signals (green), indicating the presence of a *ROS1* rearrangement. In the fusion assay, a fusion signal (yellow) was observed in the representative tumor cell of each subject, which is consistent with the presence of t(1;6)(q21.2;q22) for *TPM3-ROS1*, t(6;20)(q22;q12) for *SDC4-ROS1*, t(4;6)(q15.2;q22) for *SLC34A2-ROS1*, t(5;6)(q32;q22) for *CD74-ROS1*, inv(6)(q22q25.3) for *EZR-ROS1* or t(6;12)(q22;q14.1) for *LRIG3-ROS1*. (**b**) The break points of ROS1 are exons 32, 34 and 35. All of the break points allow the resulting fusion to harbor the kinase domain of ROS1 (red), and the exon 32 break point allows the resulting fusion to harbor the transmembrane domain of ROS1 (orange). In the fusion partners, dark blue and orange represent coiled-coil and transmembrane domains, respectively. Coiled-coil domains may contribute to homodimelization, but only TPM3 and EZR contained these domains. In contrast to ALK and RET fusions, the role of the fusion partner's coiled-coil domain is unknown in ROS1 fusions. e, exon. (**c**) Results for fusion-specific RT-PCR for tumors ROS#1 (lane 1, TPM3-ROS1, T8;R35, predicted product size of 119 bp), ROS#3 (lane 2, SDC4-ROS1, S2;R32, 596 bp), ROS#6 (lane 3, SLC34A2-ROS1, S13del2046;R32 and S13del2046;R34, 544 bp and 235 bp, respectively), ROS#8 (lane 4, CD74-ROS1, C6;R34, 230 bp), ROS#10 (lane 5, EZR-ROS1, E10;R34, 527 bp), and ROS#12 (lane 6, LRIG3-ROS1, L16;R35, 218 bp). M and N represent the size marker (100-bp ladder) and the non-template control, respectively. (**d**) The transforming potential of the ROS1 fusion. Mouse 3T3 fibroblasts infected with a retrovirus encoding SDC4-ROS1 derived from tumor ROS#4 formed multiple foci (scale bar, 1 mm). All of the four nude mice injected with the corresponding 3T3 cells developed a subcutaneous tumor (right).

(tumor RET#11). *RET* split FISH on the tissue arrays identified 22 fusion-positive tumors in 1,528 lung cancers (**Fig. 2a**), from which a multiplex RT-PCR system that captures all possible *KIF5B-RET* fusions detected 12 fusion-positive tumors: eight tumors with the fusion of *KIF5B* exon 15 and *RET* exon 12 (K15;R12) and one tumor each with the K16;R12, K22;R12, K23;R12 and K24;R11 fusions (**Fig. 2b** and **Supplementary Table 1**). The *KIF5B-RET* fusion FISH results were consistent with the presence of inv(10)(p11.22q11.2) in all 12 of these tumors (**Fig. 2a**).

In a routine histopathological diagnosis, we encountered an adenocarcinoma that showed a mucinous cribriform pattern (**Fig. 2c**) that was previously reported as a histopathological marker for the presence of EML4-ALK (**Supplementary Fig. 4**)[9–11]. Notably, this adenocarcinoma (tumor RET#14) was negative for ALK fusion and was positive for *CCDC6-RET*, as determined by FISH and inverse RT-PCR; the latter fusion gene was first described in thyroid cancer[12]. RT-PCR identified another tumor positive for the *CCDC6-RET* fusion (RET#13) in the remaining 10 tumors. The 14 RET-positive tumors (out of the total 1,528 tumors tested, with one additional tumor (RET#14) found through routine pathology diagnostic service) were also positive in the revised multiplex RT-PCR that captured *EML4-ALK*, *KIF5B-ALK*, *KIF5B-RET* and *CCDC6-RET* simultaneously (**Fig. 2d**). The RET kinase domain expression using real-time RT-PCR was weak or undetectable for the remaining nine tumors determined to be positive in the *RET* split FISH screening. Perhaps the genomic rearrangement occurred downstream of the *RET* break points. *RET* split FISH screening failed in three NSCLCs, including two adenocarcinomas. RET#14 was the index case found in routine pathology diagnostic service but not in the 1,528 cohort. RET fusions existed in 0.9% (13 out of 1,482) of the NSCLCs and 1.2% (13 out of 1,119) of the adenocarcinomas. The 14 RET fusion-positive subjects did not receive vandetanib.

We concluded that the rearrangements described above are somatic without using any matched normal tissues. Our histopathology-based screening method preserves the samples' histological architecture. This allows observers to confirm that internal non-tumor cells, for example, epithelial cells, inflammatory cells or fibroblasts, are negative in a test of interest.

All 71 kinase-fusion–positive (44 ALK, 13 ROS1 and 14 RET fusions) lung cancers were exclusively adenocarcinomas (6% of all adenocarcinomas in the present study), were positive for antibodies to TTF1, which is regarded as a marker for lung adenocarcinoma, as determined by immunohistochemistry (excluding two ALK-positive tumors) and were negative for *EGFR* and *KRAS* mutations. Thirteen of the 44 ALK-positive tumors (30%) were weakly positive for p63 expression (were weakly positive for a squamous cell carcinoma marker, p63) (**Supplementary Table 1**). Thirty-three tumors showed a mucinous cribriform pattern in at least 5% of their area; 22 tumors had this pattern in >25% of their area (**Fig. 2c**, **Supplementary Table 1** and **Supplementary Fig. 4**). The frequency of mucinous cribriform carcinoma was significantly higher in the kinase-fusion–positive group of tumors than in the 77 fusion-negative adenocarcinomas (22 out of 71 compared to 7 out of 77, respectively; $P = 0.00088$). Notably, we observed this pattern preferentially in EML4-ALK–positive tumors (70%, 29 out of 41); all three CD74-ROS1–positive tumors also showed this pattern. Recognizing this pattern in routine pathology diagnoses led to the identification of the CCDC6-RET fusion (tumor RET#14). In organs other than the lung, secretory breast carcinoma, which is characterized by a cribriform pattern with abundant secretory material, harbors the ets variant 6 (ETV6)-neurotrophic tyrosine kinase, receptor, type 3 (NTRK3) fusion (ref. 13). We identified an ALK-fusion–positive renal cell carcinoma that showed a mucinous cribriform pattern[7]. This pattern may be linked to the presence of particular kinase fusions[10], and this possibility warrants further study.

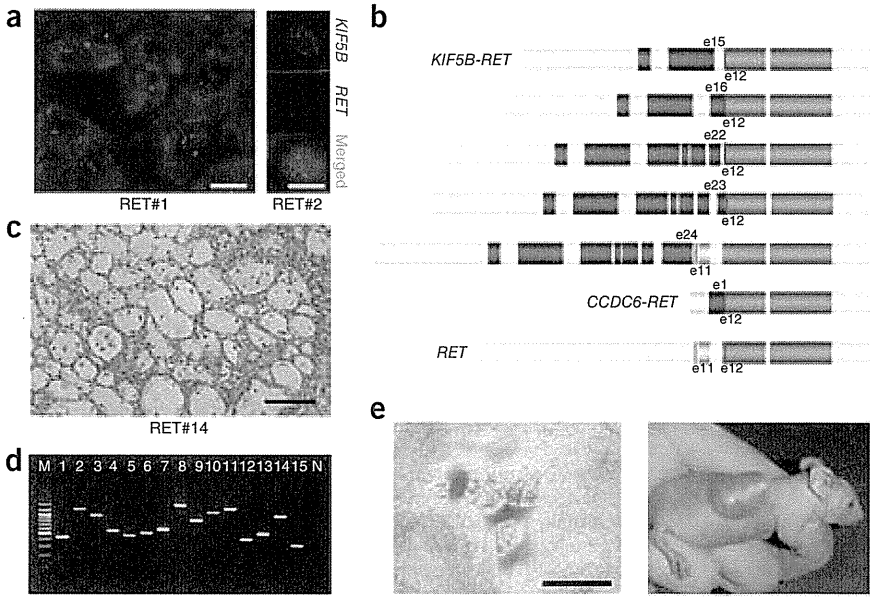

Figure 2 Discovery of RET fusions. (**a**) *RET* split (left) and fusion (right) FISH assay data (scale bars, 20 μm). In the split assay, multiple tumor cells harbored individual 3′ side signals (green), indicating the presence of *RET* rearrangement. In the fusion assay, a fusion signal (yellow) was observed in the representative tumor cell of subject RET#2, which is consistent with the presence of inv(10)(p11.22q11.2). (**b**) The break points of RET are exons 11 and 12. Both of the break points allow the resulting fusion to harbor the kinase domain of RET (red), and the exon 11 break point allows the resulting fusion to harbor the transmembrane domain of RET (orange). In the fusion partners, dark blue represents a coiled-coil domain, which probably contributes to the homodimelization of the fusion. Only the longer isoforms of RET and the RET fusions are shown. (**c**) Subject RET#14 showed the representative histopathology of mucinous cribriform carcinoma (scale bar, 100 μm). (**d**) The results for fusion-specific RT-PCR for subjects ALK#10 (lane 1, EML4-ALK, E13;A20, predicted product size of 432 bp), ALK#16 (lane 2, EML4-ALK, E20;A20, 1185 bp), ALK#26 (lane 3, EML4-ALK, E6;A20, 913 bp), ALK#38 (lane 4, EML4-ALK, E14;ins11del49A20, 546 bp), ALK#39 (lane 5, EML4-ALK, E2;A20, 454 bp), ALK#40 (lane 6, EML4-ALK, E13;ins69A20, 501 bp), ALK#41 (lane 7, EML4-ALK, E14;del14A20, 570 bp), ALK#42 (lane 8, KIF5B-ALK, K17;A20, 1,483 bp), ALK#44 (lane 9, KIF5B-ALK, K24;A20, 814 bp), RET#6 (lane 10, KIF5B-RET, K15;R12, 1,104 bp), RET#9 (lane 11, KIF5B-RET, K16;R12, 1,293 bp), RET#10 (lane 12, KIF5B-RET, K22;R12, 420 bp), RET#11 (lane 13, KIF5B-RET, K23;R12, 525 bp), RET#12 (lane 14, KIF5B-RET, K24;R11, 999 bp) and RET#13 (lane 15, CCDC6-RET, C1;R12, 352 bp). M and N represent the size marker (100-bp ladder) and non-template control, respectively. (**e**) The transforming potential of the KIF5B-RET fusion. Mouse 3T3 fibroblasts infected with a retrovirus encoding K15;R12L derived from tumor RET#7 fomed multiple foci (scale bar, 1 mm). All of the four nude mice injected with the corresponding 3T3 cells developed a subcutaneous tumor (right).

Supplementary Tables 1–4 summarize the clinicopathological features of the subjects. Briefly, young age, low smoking index and small tumor size characterized the kinase-fusion–positive group of subjects (**Supplementary Table 2**). A multivariate analysis of the adenocarcinomas revealed four independent factors that were indicators of poor prognosis: age ≥50 years, male sex, high pathological stage and negative kinase-fusion status (**Supplementary Table 3**). There was no significant difference in overall survival between the kinase-positive and epidermal growth factor receptor (EGFR)-mutant groups (P = 0.32). **Supplementary Table 4** shows the clinicopathological features of the subjects stratified by each fusion.

The transforming ability of CCDC6-RET and all of the ALK fusions, excluding K17;A20, was shown previously[1–3,8,12]. 3T3 cells infected with a virus expressing K17;A20, tropomyosin 3 (TPM3)-ROS1, syndecan 4 (SDC4)-ROS1, SLC34A2-ROS1, CD74-ROS1, ezrin (EZR)-ROS1, leucine-rich repeats and immunoglobulin-like domains 3 (LRIG3) (transcript variant 2)-ROS1 or KIF5B-RET (with both the longer (RET51) and shorter (RET9) RET isoforms) led to multiple transformed foci formation in culture and in subcutaneous tumors in a nude mouse tumorigenicity assay (**Figs. 1d, 2e** and **Supplementary Fig. 5**).

To test whether vandetanib, an inhibitor of vascular endothelial growth factor receptor (VEGFR-2), VEGFR-3, EGFR and RET[14], might be effective for the treatment of RET-fusion–positive tumors, we induced Flag-tagged EML4-ALK (E13;A20) or KIF5B-RET (K15;R12L and K15;R12S) in Ba/F3 cells, which are dependent on interleukin-3 (IL-3) for growth. All transfected cells, including those without any kinase fusion, proliferated in the presence of IL-3, but only cells expressing E13;A20 or K15;R12L grew in the absence of IL-3 (**Supplementary Fig. 6a**). In the absence of IL-3, vandetanib inhibited the proliferation of cells expressing K15;R12L (**Supplementary Fig. 6c**) but not the proliferation of cells expressing E13;A20 (**Supplementary Fig. 6d**). Crizotinib was not effective in inhibiting the proliferation of Ba/F3 cells expressing K15;R12L (**Supplementary Fig. 7**).

In 1985, a 3T3 assay identified *RET* as a rearranged transforming gene[15]. RET fusions have been identified exclusively in papillary thyroid carcinoma and are more frequently observed in radiation-associated thyroid cancers (for example, in survivors of the Chernobyl accident[16], atomic bomb survivors[17] and post-radiation therapy patients[18]). Therefore, a retrospective comparison of RET fusions in individuals with lung cancer with and without a history of radiation exposure warrants further study. If a positive association is found between RET fusion and radiation exposure in these studies, it might be desirable for individuals with internal or therapeutic exposure to irradiation (for example, those individuals involved in the Fukushima accident) to be monitored prospectively for lung cancer as well as thyroid cancer.

In Japan, more than 40% of lung adenocarcinomas in younger individuals harbor EGFR mutations[19]. In this study, 16% (17 out of 107) of younger individuals (≤50 years of age) with adenocarcinoma harbored a kinase fusion. Collectively, as long as molecular target diagnoses are properly performed, >50% of the individuals with lung adenocarcinoma in this generation may benefit from treatment with corresponding kinase inhibitors. Integrated pathology-based screening techniques can also be used for the selection of individuals to receive this treatment[20]. The results of our study will facilitate the development of a molecular classification of lung adenocarcinomas that is closely related to both the pathogenesis and the treatment of disease. This study was approved by the Institutional Review Board of the Cancer Institute Hospital, and all subjects provided informed consent.

METHODS

Methods and any associated references are available in the online version of the paper at http://www.nature.com/naturemedicine/.

Note: Supplementary information is available on the Nature Medicine website.

ACKNOWLEDGMENTS

We thank M. Iwakoshi, K. Shiozawa, T. Kakita, H. Nagano and K. Nomura for their technical assistance and S. Sengoku for providing administrative assistance. This work was supported in part by Grants-in-Aid for Scientific Research from the Ministry of Education, Culture, Sports, Science and Technology of Japan, as well as by grants from the Japan Society for the Promotion of Science; the Ministry of Health, Labor and Welfare of Japan; the Vehicle Racing Commemorative Foundation of Japan; the Princess Takamatsu Cancer Research Fund; and the Uehara Memorial Foundation.

AUTHOR CONTRIBUTIONS

K.T. conceived of and led the entire project, designed the FISH probes, screened samples using FISH and immunohistochemistry, performed histopathological analyses, generated figures and tables and wrote the manuscript. M.S. performed functional analyses and generated the figures. Y.T. performed inverse RT-PCR and RACE experiments and their corresponding analyses. R.S. conducted statistical analyses. S.S. performed FISH and histopathological analyses. S.H. processed and analyzed the tissue microarrays and FISH screening and generated figures. R.A. processed the FISH probe library. W.H. made and analyzed the database and processed tissue microarrays. H.N., H.U., Y.S., S.O. and K.N. collected specimens and clinical information and were involved in planning the project. Y.L.C. conducted functional analyses. H.M. supervised the functional analyses and planned the project. Y.I. performed histopathological analyses and collected specimens. All authors participated in the discussion and interpretation of the data and the results.

COMPETING FINANCIAL INTERESTS

The authors declare no competing financial interests.

Published online at http://www.nature.com/naturemedicine/.
Reprints and permissions information is available online at http://www.nature.com/reprints/index.html.

1. Soda, M. *et al. Nature* **448**, 561–566 (2007).
2. Takeuchi, K. *et al. Clin. Cancer Res.* **14**, 6618–6624 (2008).
3. Takeuchi, K. *et al. Clin. Cancer Res.* **15**, 3143–3149 (2009).
4. Rikova, K. *et al. Cell* **131**, 1190–1203 (2007).
5. Takeuchi, K. *et al. Haematologica* **96**, 464–467 (2011).
6. Takeuchi, K. *et al. Clin. Cancer Res.* **17**, 3341–3348 (2011).
7. Sugawara, E. *et al. Cancer* published online, doi:10.1002/cncr.27391 (17 January 2012).
8. Choi, Y.L. *et al. Cancer Res.* **68**, 4971–4976 (2008).
9. Inamura, K. *et al. J. Thorac. Oncol.* **3**, 13–17 (2008).
10. Takeuchi, K. *Pathol. and Clin. Med.* **28**, 139–144 (2010).
11. Jokoji, R. *et al. J. Clin. Pathol.* **63**, 1066–1070 (2010).
12. Grieco, M. *et al. Cell* **60**, 557–563 (1990).
13. Tognon, C. *et al. Cancer Cell* **2**, 367–376 (2002).
14. Flanigan, J., Deshpande, H. & Gettinger, S. *Biologics* **4**, 237–243 (2010).
15. Takahashi, M., Ritz, J. & Cooper, G.M. *Cell* **42**, 581–588 (1985).
16. Ito, T. *et al. Lancet* **344**, 259 (1994).
17. Hamatani, K. *et al. Cancer Res.* **68**, 7176–7182 (2008).
18. Bounacer, A. *et al. Oncogene* **15**, 1263–1273 (1997).
19. Kosaka, T. *et al. Cancer Res.* **64**, 8919–8923 (2004).
20. Han, B. *et al. Cancer Res.* **68**, 7629–7637 (2008).

Original Article

Identification of Anaplastic Lymphoma Kinase Fusions in Renal Cancer

Large-Scale Immunohistochemical Screening by the Intercalated Antibody-Enhanced Polymer Method

Emiko Sugawara, MD[1,2]; Yuki Togashi, MS[1,3]; Naoto Kuroda, MD[4]; Seiji Sakata, MD, PhD[1]; Satoko Hatano, BS[1,3]; Reimi Asaka, BS[1,3]; Takeshi Yuasa, MD, PhD[5]; Junji Yonese, MD, PhD[5]; Masanobu Kitagawa, MD, PhD[2]; Hiroyuki Mano, MD, PhD[6,7]; Yuichi Ishikawa, MD, PhD[3]; and Kengo Takeuchi, MD, PhD[1,3]

BACKGROUND: Several promising molecular-targeted drugs are used for advanced renal cancers. However, complete remission is rarely achieved, because none of the drugs targets a key molecule that is specific to the cancer, or is associated with "oncogene addiction" (dependence on one or a few oncogenes for cell survival) of renal cancer. Recently, an anaplastic lymphoma kinase (ALK) fusion, vinculin-ALK, has been reported in pediatric renal cell carcinoma (RCC) cases who have a history of sickle cell trait. In this context, ALK inhibitor therapy would constitute a therapeutic advance, as has previously been demonstrated with lung cancer, inflammatory myofibroblastic tumors, and anaplastic large cell lymphomas. **METHODS:** Anti-ALK immunohistochemistry was used to screen 355 tumor tissues, using the intercalated antibody-enhanced polymer (iAEP) method. The cohort consisted of 255 clear cell RCCs, 32 papillary RCCs, 34 chromophobe RCCs, 6 collecting duct carcinomas, 10 unclassified RCCs, 6 sarcomatoid RCCs, and 12 other tumors. **RESULTS:** Two patients (36- and 53-year-old females) were positive for ALK as determined by iAEP immunohistochemistry. Using 5′-rapid amplification of complementary DNA ends, we detected *TPM3-ALK* and *EML4-ALK* in these tumors. The results of this study were confirmed by fluorescence in situ hybridization assays. The 2 ALK-positive RCCs were unclassified (mixed features of papillary, mucinous cribriform, and solid patterns with rhabdoid cells) and papillary subtype. They comprised 2.3% of non-clear cell RCCs (2 of 88) and 3.7% of non-clear cell and nonchromophobe RCCs (2 of 54). **CONCLUSIONS:** The results of this study indicate that ALK fusions also exist in adult RCC cases without uncommon backgrounds. These findings confirm the potential of ALK inhibitor therapy for selected cases of RCC. *Cancer* **2012;000:000-000.** © *2012 American Cancer Society.*

KEYWORDS: anaplastic lymphoma kinase, molecular-targeted therapy, renal cell carcinoma, immunohistochemistry, intercalated antibody-enhanced polymer.

INTRODUCTION

Renal cancer is one of the major cancers. The incidence and mortality of cases are estimated at 273,518 and 116,368 in the world; 14,963 and 6957 in Japan; and 56,678 and 13,711 in the United States.[1] The 5-year survival rate of patients with localized disease is relatively good: 65% to 93% and 47% to 77% for stages 1 and 2, respectively.[2] For advanced renal cancers (34%-80% and 2%-20% 5-year survival rates in stages 3 and 4, respectively),[2] several molecular-targeted drugs have been recently approved by the US Food and Drug Administration. These drugs, which include sunitinib, sorafenib, temsirolimus, everolimus, bevacizumab, pazopanib, and axitinib, are promising. However, none of them targets a key molecule that is specific to the cancer, or is associated with "oncogene addiction" of renal cancer, namely, the dependence on one or a few oncogenes for maintenance of the malignant phenotype and cell survival.

Anaplastic lymphoma kinase (ALK) fusion is a potential vulnerability, an "Achilles' heel", of many types of human cancer, including lymphoma,[3,4] sarcoma,[5] and carcinoma.[6,7] Experimentally, lung adenocarcinomas developed in EML4-ALK (fusion of ALK with echinoderm microtubule–associated protein like 4) transgenic mice were successfully treated with an ALK inhibitor.[8] The ALK inhibitor crizotinib has recently been used in patients with lung cancer, inflammatory myofibroblastic tumors (IMTs), or anaplastic large cell lymphomas (ALCLs), which harbor various ALK fusions. The compound showed an 81% response rate in ALK-positive lung cancers defined by at least 2 diagnostic methods,[9,10] and a

Corresponding author: Kengo Takeuchi, MD, PhD, Pathology Project for Molecular Targets, The Cancer Institute, Japanese Foundation for Cancer Research, 3-8-31 Ariake, Koto, Tokyo 135-8550, Japan; Fax: (81) 3-3570-0230; kentakeuchi-tky@umin.net

[1]Pathology Project for Molecular Targets, The Cancer Institute, Japanese Foundation for Cancer Research, Tokyo, Japan; [2]Department of Comprehensive Pathology, Graduate School, Tokyo Medical and Dental University, Tokyo, Japan; [3]Division of Pathology, The Cancer Institute, Japanese Foundation for Cancer Research, Tokyo, Japan; [4]Department of Diagnostic Pathology, Kochi Red Cross Hospital, Kochi City, Kochi, Japan; [5]Department of Urology, The Cancer Institute Hospital, Japanese Foundation for Cancer Research, Tokyo, Japan; [6]Division of Functional Genomics, Jichi Medical University, Tochigi, Japan; [7]Department of Medical Genomics, Graduate School of Medicine, University of Tokyo, Tokyo, Japan

We thank Tomoyo Kakita, Keiko Shiozawa, and Motoyoshi Iwakoshi for their technical assistance, and Sayuri Sengoku for providing administrative assistance.

DOI: 10.1002/cncr.27391, **Received:** October 1, 2011; **Revised:** October 31, 2011; **Accepted:** November 10, 2011, **Published online** in Wiley Online Library (wileyonlinelibrary.com)

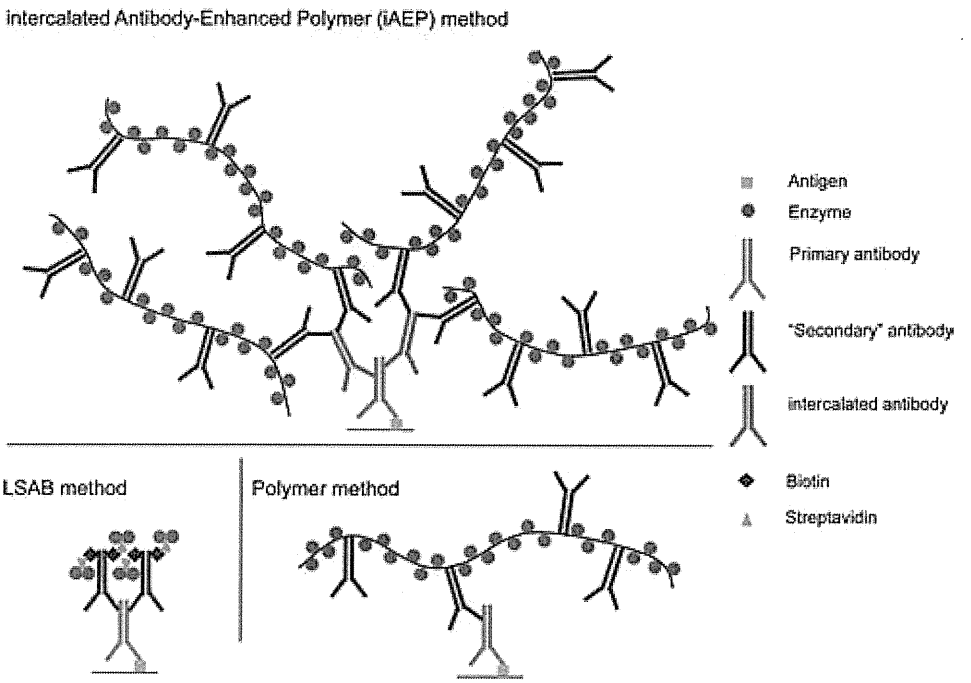

Figure 1. Schematic of intercalated antibody-enhanced polymer (iAEP) method is shown. The labeled streptavidin biotin (LSAB) and polymer methods are common conventional immunohistochemistry methods. In the iAEP method, a step of "intercalated antibody" is added between those of the primary antibody and polymer reagent. Thus, the iAEP method has an additional step compared with the polymer method, but the same number of steps as the LSAB method. There are generally 2 ways to raise the sensitivity of immunohistochemistry. The first is to raise the sensitivity of the antigen-antibody reaction, by increasing the concentration of the primary antibody, using a more sensitive antibody, antigen-retrieval technique, and so forth. The second is to raise the sensitivity of the detection system for the antigen-antibody immune complex. These 2 techniques may appear to generate the same result; however, in principle, they are totally different. The staining results are more likely to differ, especially when the antigen density is very low, such as for EML4-ALK (fusion of echinoderm microtubule-associated protein like 4 with anaplastic lymphoma kinase) or PPFIBP1-ALK (fusion of PTPRF interacting protein binding protein 1 with ALK).[13,24] In such a setting, the latter technique is more advantageous. The staining intensity depends on the density of enzyme in the antigen site. However sensitive a primary antibody is, the antigen-antibody complex cannot exceed the number of antigens. In contrast, it is easy to increase the enzyme density per antigen-antibody complex with use of the latter technique, which includes the iAEP method.

strong response in IMT for several months.[11] Two patients with ALCL who were receiving crizotinib achieved complete remission.[12] These findings indicate that ALK fusion addiction is one of the most promising targets in cancer therapy.

To ensure that such molecular-targeted therapy is effective and less toxic, accurate screening methods to detect ALK fusions are crucial. However, although immunohistochemistry has been a gold standard for the detection of ALK fusions in ALCL and IMT,[13,14] conventional anti-ALK immunohistochemistry is not sensitive enough to detect EML4-ALK, which was first described in lung cancer in 2007.[6,7] To overcome this, we developed a sensitive immunohistochemical tool, the intercalated antibody-enhanced polymer (iAEP) method (Fig. 1).[13] Combined with a conventional anti-ALK mouse monoclonal antibody 5A4, the iAEP method efficiently and consistently detected EML4-ALK in paraffin-embedded sections. In various studies on ALK-positive lung cancer, anti-ALK immunohistochemistry by iAEP or essentially equivalent methods was used to examine surgically resected specimens,[13,15-19] transbronchial lung biopsy specimens,[20] and endobronchial ultrasound-guided transbronchial needle aspiration specimens.[17,21,22] More importantly, some of the patients screened by anti-ALK iAEP immunohistochemical analysis received crizotinib therapy and showed a good response.[16,17,22] Novel ALK fusions, including v6 and v7 of EML4-ALK,[13] kinesin family member 5B (KIF5B)-ALK,[13] sequestosome 1 (SQSTM1)-ALK,[23] and PTPRF interacting protein, binding protein 1 (PPFIBP1)-ALK[24] have been identified using anti-ALK iAEP immunohistochemical analysis. Thus, anti-ALK iAEP immunohistochemistry constitutes a powerful tool for clinical and also research purposes.

The development of anti-ALK antibodies has facilitated the investigation of many types and cases of cancer, including lung cancer.[25-27] Since 1994, ALK-positive tumors have been identified exclusively in lymphoma